

Information Theoretic Regret Bounds for Online Nonlinear Control

Sham Kakade^{1,2}, Akshay Krishnamurthy²,
Kendall Lowrey¹, Motoya Ohnishi¹, and Wen Sun²

¹University of Washington

²Microsoft Research NYC

June 23, 2020

Abstract

This work studies the problem of sequential control in an unknown, *nonlinear* dynamical system, where we model the underlying system dynamics as an unknown function in a known Reproducing Kernel Hilbert Space. This framework yields a general setting that permits discrete and continuous control inputs as well as non-smooth, non-differentiable dynamics. Our main result, the Lower Confidence-based Continuous Control (LC³) algorithm, enjoys a near-optimal $O(\sqrt{T})$ regret bound against the optimal controller in episodic settings, where T is the number of episodes. The bound has *no* explicit dependence on dimension of the system dynamics, which could be infinite, but instead only depends on information theoretic quantities. We empirically show its application to a number of *nonlinear* control tasks and demonstrate the benefit of exploration for learning model dynamics.

1 Introduction

The control of uncertain dynamical systems is one of the central challenges in Reinforcement Learning (RL) and continuous control, and recent years has seen a number of successes in demanding sequential decision making tasks ranging from robotic hand manipulation [Todorov et al., 2012, Al Borno et al., 2012, Kumar et al., 2016, Tobin et al., 2017, Lowrey et al., 2018, Akkaya et al., 2019] to game playing [Silver et al., 2016, Bellemare et al., 2016, Pathak et al., 2017, Burda et al., 2018]. The predominant approaches here are either based on reinforcement learning or continuous control (or a mix of techniques from both domains).

With regards to provably correct methods which handle both the learning and approximation in unknown, complex environments, the body of results in the reinforcement learning literature [Russo and Van Roy, 2013, Jiang et al., 2017, Sun et al., 2019, Agarwal et al., 2019a] is

far more mature than in the continuous controls literature. In fact, only relatively recently has there been provably correct methods (and sharp bounds) for the learning and control of the Linear Quadratic Regulator (LQR) model [Mania et al., 2019, Simchowicz and Foster, 2020, Abbasi-Yadkori and Szepesvári, 2011], arguably the most basic model due to having globally *linear* dynamics.

While Markov Decision Processes provide a very general framework after incorporating continuous states and actions into the model, there are a variety of reasons to directly consider learning in continuous control settings: even the simple LQR model provides a powerful framework when used for *locally* linear planning [Ahn et al., 2007, Todorov and Li, 2005, Tedrake, 2009, Perez et al., 2012]. More generally, continuous control problems often have continuity properties with respect to the underlying “disturbance” (often modeled as statistical additive noise), which can be exploited for fast path planning algorithms [Jacobson and Mayne, 1970, Williams et al., 2017]; analogous continuity properties are often not leveraged in designing provably correct RL models (though there are a few exceptions, e.g. [Kakade et al., 2003]). While LQRs are a natural model for continuous control, they are prohibitive for a variety of reasons: LQRs rarely provide good *global* models of the system dynamics, and, furthermore, naive random search suffices for sample efficient learning of LQRs [Mania et al., 2019, Simchowicz and Foster, 2020] — a strategy which is unlikely to be effective for the learning and control of more complex nonlinear dynamical systems where one would expect strategic exploration to be required for sample efficient learning (just as in RL, e.g. see Kearns and Singh [2002], Kakade [2003]).

This is the motivation for this line of work, where we focus directly on the sample efficient learning and control of an *unknown*, nonlinear dynamical system, under the assumption that the mean dynamics live within some known Reproducing Kernel Hilbert Space.

The Online Nonlinear Control Problem. This work studies the following nonlinear control problem, where the nonlinear system dynamics are described, for $h \in \{0, 1, \dots, H - 1\}$, by

$$x_{h+1} = f(x_h, u_h) + \epsilon, \text{ where } \epsilon \sim \mathcal{N}(0, \sigma^2 I)$$

where the state $x_h \in \mathbb{R}^{d_x}$; the control $u_h \in \mathcal{U}$ where \mathcal{U} may be an arbitrary set (not necessarily even a vector space); $f : \mathcal{X} \times \mathcal{U} \rightarrow \mathcal{X}$ is assumed to live within some known Reproducing Kernel Hilbert Space; the additive noise is assumed to be independent across timesteps.

Specifically, the model considered in this work was recently introduced in Mania et al. [2020], which we refer to as the *kernelized nonlinear regulator* (KNR) for the infinite dimensional extension. The KNR model assumes that f lives in the RKHS of a known kernel K . Equivalently, the primal version of this assumption is that:

$$f(x, u) = W^* \phi(x, u)$$

for some known function $\phi : \mathcal{X} \times \mathcal{U} \rightarrow \mathcal{H}$ where \mathcal{H} is a Hilbert space (either finite or countably infinite dimensional) and where W^* is a linear mapping. Given an immediate cost function $c : \mathcal{X} \times \mathcal{U} \rightarrow \mathbb{R}^+$ (where \mathbb{R}^+ is the non-negative real numbers), the KNR problem can be described

by the following optimization problem:

$$\min_{\pi \in \Pi} J^\pi(x_0; c) \text{ where } J^\pi(x_0; c) = \mathbb{E} \left[\sum_{h=0}^{H-1} c(x_h, u_h) \middle| \pi, x_0 \right]$$

where x_0 is a given starting state; Π is some set of feasible controllers; and where a controller (or a policy) is a mapping $\pi : \mathcal{X} \times \{0, \dots, H-1\} \rightarrow \mathcal{U}$. We denote the best-in-class cumulative cost as $J^*(x_0; c) = \min_{\pi \in \Pi} J^\pi(x_0; c)$. Given any model parameterization W , we denote $J^\pi(x_0; c, W)$ as the expected total cost of π under the dynamics $W\phi(x, u) + \epsilon$.

It is worthwhile to note that this KNR model is rather general in the following sense: the space of control inputs \mathcal{U} may be either discrete or continuous; and the dynamics f need not be a smooth or differentiable function in any of its inputs. A more general version of this problem, which we leave for future work, would be where the systems dynamics are of the form $x_{h+1} = f_h(x_h, u_h, \epsilon_h)$, in contrast to our setting where the disturbance is due to additive Gaussian noise.

We consider an online version of this KNR problem: the objective is to sequentially optimize a sequence of cost functions where the nonlinear dynamics f are not known in advance. We assume that the learner knows the underlying Reproducing Kernel Hilbert Space. In each episode t , we observe an instantaneous cost function c^t ; we choose a policy π^t ; we execute π^t and observe a sampled trajectory $x_0, u_0, \dots, x_{H-1}, u_{H-1}$; we incur the cumulative cost under c^t . Our goal is to minimize the sum of our costs over T episodes. In particular, we desire to execute a policy that is nearly optimal for every episode.

A natural performance metric in this context is our cumulative regret, the increase in cost due to not knowing the nonlinear dynamics beforehand, defined as:

$$\text{REGRET}_T = \sum_{t=0}^{T-1} \sum_{h=0}^{H-1} c^t(x_h^t, u_h^t) - \sum_{t=0}^{T-1} \min_{\pi \in \Pi} J^\pi(x_0; c^t)$$

where $\{x_h^t\}$ is the observed states and $\{u_h^t\}$ is the observed sequence of controls. A desirable asymptotic property of an algorithm is to be no-regret, i.e. the time averaged version of the regret goes to 0 as T tends to infinity.

Our Contributions. The first set of provable results in this setting, for the finite dimensional case and for the problem of system identification, was provided by [Mania et al. \[2020\]](#). Our work focuses on regret, and we provide the Lower Confidence-based Continuous Control (LC³) algorithm, which enjoys a $O(\sqrt{T})$ regret bound. We provide an informal version of our main result, specialized to the case where the dimension of the RKHS is finite and the costs are bounded.

Theorem 1.1 (Informal statement; finite dimensional case with bounded features). *Consider the special case where: $c^t(x, u) \in [0, 1]$; d_ϕ is finite (with $d_{\mathcal{X}} + d_\phi \geq H$); and ϕ is uniformly bounded, with $\|\phi(x, u)\|_2 \leq B$; The LC³ algorithm enjoys the following expected regret bound:*

$$\mathbb{E}_{\text{LC}^3} [\text{REGRET}_T] \leq \tilde{O} \left(\sqrt{d_\phi(d_{\mathcal{X}} + d_\phi)H^3T} \cdot \log \left(1 + \frac{B^2\|W^*\|_2^2}{\sigma^2} \right) \right),$$

where $\tilde{O}(\cdot)$ notation drops logarithmic factors in T and H .

There are a number of notable further contributions with regards to our work:

- (*Dimension and Horizon Dependencies*) Our general regret bound has *no* explicit dependence on dimension of the system dynamics (the RKHS dimension), which could be infinite, but instead only depends on information theoretic quantities; our horizon dependence is H^3 , which we conjecture is near optimal. It is also worthwhile noting that our regret bound is only logarithmic in $\|W^*\|_2$ and σ^2 .
- (*Localized rates*) In online learning, it is desirable to obtain improved rates if the loss of the “best expert” is small, e.g. in our case, if $J^*(x_0; c^t)$ is small. Under a bounded coefficient of variation condition (which holds for LQRs and may hold more generally), we provide an improved regret bound whose leading term regret depends linearly on J^* .
- (*Moment bounds and LQRs*) Our regret bound does not require bounded costs, but instead only depends on second moment bounds of the realized cumulative cost, thus making them applicable to LQRs, as a special case.
- (*Empirical evaluation:*) Coupled with the right features (e.g., kernels), our method, arguably one of the simplest, provides competitive results in common continuous control benchmarks, exploration tasks, and complex control problems such as dexterous manipulation.

While our techniques utilize methods developed for the analysis of linear bandits [Dani et al., 2008, Abbasi-Yadkori et al., 2011] and Gaussian process bandits [Srinivas et al., 2009], there are a number of new technical challenges to be addressed with regards to the multi-step extension to Reinforcement Learning. In particular, some nuances for the more interested reader: we develop a stopping time martingale to handle the unbounded nature of the (realized) cumulative costs; we develop a novel way to handle Gaussian smoothing through the chi-squared distance function between two distributions; our main technical lemma is a “self-bounding” regret bound that relates the instantaneous regret on any given episode to the second moment of the stochastic process.

Notation. We let $\|x\|_2$, $\|M\|_2$, and $\|M\|_F$ refer to the Euclidean norm, the spectral norm, and the Frobenius norm, respectively, of a vector x and a matrix M .

2 Related Work

The first set of provable results with regards to this nonlinear control model was provided by Mania et al. [2020], who studied the problem of system identification in a finite dimensional setting (we discuss these results later). While not appearing with this name, a Gaussian process version of this model was originally considered by Deisenroth and Rasmussen [2011], without sample-efficiency guarantees.

More generally, most model-based RL/controls algorithms do not explicitly address the exploration challenge nor do they have guarantees on the performance of the learned policy [Deisenroth and Rasmussen, 2011, Levine and Abbeel, 2014, Chua et al., 2018, Kurutach et al., 2018, Nagabandi et al., 2018, Luo et al., 2018, Ross and Bagnell, 2012]. Departing from these works, we

focus on provable sample efficient regret bounds and strategic exploration in model-based learning in the kernelized nonlinear regulator.

Among provably efficient model-based algorithms, works from [Sun et al. \[2019\]](#), [Osband and Van Roy \[2014\]](#), [Ayoub et al. \[2020\]](#), [Lu and Van Roy \[2019\]](#) are the most related to our work. While these works are applicable to certain linear structures, their techniques do not lead to the results herein: even for the special case of LQRs, they do not address the unbounded nature of the costs, where there is more specialized analysis [[Mania et al., 2019](#), [Cohen et al., 2019](#), [Simchowitz and Foster, 2020](#)]; these results do not provide techniques for sharp leading order dependencies like in our regret results (and the former three do not handle the infinite dimensional case); they also do not provide techniques for localized regret bounds, like those herein which depend on J^* . A few more specific differences: the model complexity measure Witness Rank from [Sun et al. \[2019\]](#) does contain the kernelized nonlinear regulator if the costs were bounded and the dimensions were finite; [Osband and Van Roy \[2014\]](#) considers a setting where the model class has small Eluder dimension, which does not apply to the infinite-dimensional settings that we consider here; [Lu and Van Roy \[2019\]](#) presents a general information theoretic framework providing results for tabular and factor MDPs. There are numerous technical challenges addressed in this work which may be helpful for further analysis of models in continuous control problems.

Another family of related work provides regret analyses of online LQR problems. There are a host of settings considered: unknown stochastic dynamics [[Abbasi-Yadkori and Szepesvári, 2011](#), [Dean et al., 2018](#), [Mania et al., 2019](#), [Cohen et al., 2019](#), [Simchowitz and Foster, 2020](#)]; adversarial noise (or adversarial noise with unknown mean dynamics) [[Agarwal et al., 2019b](#), [Hazan et al., 2019](#)]; changing cost functions with known dynamics [[Cohen et al., 2018](#), [Agarwal et al., 2019c](#)]. For the case of unknown (stochastic) dynamics, our online KNR problem is more general than these works, due to a more general underlying model; one distinction is that many of these prior works on LQRs consider the regret on a single trajectory, under stronger stability and mixing assumptions of the process. This is an interesting direction for future work (see Section 5).

On the system identification side, [Mania et al. \[2020\]](#) provides the first sample complexity analysis for finite dimensional KNRs under assumptions of reachability and bounded features. The work of [Mania et al. \[2020\]](#) is an important departure from the aforementioned model-based theoretical results [[Sun et al., 2019](#), [Osband and Van Roy, 2014](#), [Ayoub et al., 2020](#), [Lu and Van Roy, 2019](#)]; the potentially explosive nature of the system dynamics makes system ID challenging, and [Mania et al. \[2020\]](#) directly addresses this through various continuity assumptions on the dynamics. One notable aspect of our work is that it permits both an unbounded state and unbounded features. The KNR also has been used in practice for system identification [[Ng et al., 2006](#), [Abbeel and Ng, 2005](#)].

3 Main Results

3.1 The Lower Confidence-based Continuous Control algorithm

LC³ is based on “optimism in the face of uncertainty,” which is described in Algorithm 1. At episode t , we use all previous experience to define an uncertainty region (an ellipse). The center

Algorithm 1 Lower Confidence-based Continuous Control (LC³)

Require: Policy class Π ; regularizer λ ; confidence parameter C_1 (see Equation 3.3).

- 1: Initialize BALL^0 to be any set containing W^* .
 - 2: **for** $t = 0 \dots T$ **do**
 - 3: $\pi^t = \arg \min_{\pi \in \Pi} \min_{W \in \text{BALL}^t} J^\pi(x_0; c^t, W)$
 - 4: Execute π^t to sample a trajectory $\tau^t := \{x_h^t, u_h^t, c_h^t, x_{h+1}^t\}_{h=0}^{H-1}$
 - 5: Update BALL^{t+1} (as specified in Equation 3.2).
 - 6: **end for**
-

of this region, \bar{W}^t , is the solution of the following regularized least squares problem:

$$\bar{W}^t = \arg \min_W \sum_{\tau=0}^{t-1} \sum_{h=0}^{H-1} \|W\phi(x_h^\tau, u_h^\tau) - x_{h+1}^\tau\|_2^2 + \lambda \|W\|_F^2, \quad (3.1)$$

where λ is a parameter, and the shape of the region is defined through the feature covariance:

$$\Sigma^t = \lambda I + \sum_{\tau=0}^{t-1} \sum_{h=0}^{H-1} \phi(x_h^\tau, u_h^\tau)(\phi(x_h^\tau, u_h^\tau))^\top, \quad \text{with } \Sigma^0 = \lambda I.$$

The uncertainty region, or confidence ball, is defined as:

$$\text{BALL}^t = \left\{ W \mid \left\| (W - \bar{W}^t) (\Sigma^t)^{1/2} \right\|_2^2 \leq \beta^t \right\}, \quad (3.2)$$

where recall that $\|M\|_2$ denotes the spectral norm of a matrix M and where

$$\beta^t := C_1 \left(\lambda \sigma^2 + \sigma^2 \left(d_{\mathcal{X}} + \log(t \det(\Sigma^t) / \det(\Sigma^0)) \right) \right), \quad (3.3)$$

with C_1 being a parameter of the algorithm.

At episode t , the LC³ algorithm will choose an optimistic policy in Line 3 of Algorithm 1. Solving this optimistic planning problem in general is NP-hard [Dani et al., 2008]. Given this computational hardness, we focus on the statistical complexity and explicitly assume access to the following computational oracle:

Assumption 1 (Black-box computation oracle). *We assume access to an oracle that implements Line 3 of Algorithm 1.*

We leave to future work the question of finding reasonable approximation algorithms, though we observe that a number of effective heuristics may be available through gradient based methods such as DDP [Jacobson and Mayne, 1970], iLQG [Todorov and Li, 2005] and CIO [Mordatch et al., 2012], or sampling based methods, such as MPPI [Williams et al., 2017] and DMD-MPC [Wagener et al., 2019]. In particular, these planning algorithms are natural to use in conjunction with Thompson Sampling [Thompson, 1933, Osband and Van Roy, 2014], i.e. we sample W^t from $\mathcal{N}(\bar{W}^t, (\Sigma^t)^{-1})$ and then compute and execute the corresponding optimal policy

$\pi^t = \arg \min_{\pi \in \Pi} J^\pi(x_0; c^t, W^t)$ using a planning oracle. While we focus on the frequentist regret bounds, we conjecture that a Bayesian regret bound for the Thompson sampling algorithm, should be achievable using the techniques we develop herein, along with now standard techniques for analyzing the Bayesian regret of Thompson sampling (e.g. see [Russo and Van Roy \[2014\]](#)).

3.2 Information Theoretic Regret Bounds

In this section, we analyze the regret of Algorithm 1. Following [Srinivas et al. \[2009\]](#), let us define the (expected) Maximum Information Gain as:

$$\begin{aligned} \gamma_T(\lambda) &:= \max_{\mathcal{A}} \mathbb{E}_{\mathcal{A}} \left[\log \left(\det(\Sigma^T) / \det(\Sigma^0) \right) \right] \\ &= \max_{\mathcal{A}} \mathbb{E}_{\mathcal{A}} \left[\log \det \left(I + \frac{1}{\lambda} \sum_{t=0}^{T-1} \sum_{h=0}^{H-1} \phi(x_h^t, u_h^t) (\phi(x_h^t, u_h^t))^\top \right) \right], \end{aligned}$$

where the max is over algorithms \mathcal{A} , where an algorithm is a mapping from the history before episode t to the next policy $\pi_t \in \Pi$.

Remark 3.1. (Finite dimensional RKHS) For $\phi \in \mathbb{R}^{d_\phi}$, with $\|\phi(x, u)\| \leq B \in \mathbb{R}^+$ for all (x, u) , then $\gamma_T(\lambda)$ will be $O(d_\phi \log(1 + THB^2/\lambda))$ (see Lemma C.5). Furthermore, it may be the case that $\gamma_T(\lambda) \ll d_\phi$ if the eigenspectrum of the covariance matrices of the policies tend to concentrate in a lower dimensional subspace. See [Srinivas et al. \[2009\]](#) for details and for how $\gamma_T(\lambda)$ scales for a number of popular kernels.

The General Case, with Bounded Moments

Assumption 2. (Bounded second moments at x_0) Assume that c^t is a non-negative function for all t and that the realized cumulative cost, when starting from x_0 , has uniformly bounded second moments, over all policies and cost functions c^t . Precisely, suppose for every c^t ,

$$\sup_{\pi \in \Pi} \mathbb{E} \left[\left(\sum_{h=0}^{H-1} c^t(x_h, u_h) \right)^2 \mid x_0, \pi \right] \leq V_{\max}.$$

This assumption is substantially weaker than the standard bounded cost assumption used in prior model-based works [[Sun et al., 2019](#), [Lu and Van Roy, 2019](#)]; furthermore, the assumption only depends on the starting x_0 as opposed to a uniform bound over the state space.

Theorem 3.2 (LC³ regret bound). Suppose Assumptions 1 and 2 hold. Set $\lambda = \frac{\sigma^2}{\|W^*\|_2^2}$ and define

$$\tilde{d}_T^2 := \gamma_T(\lambda) \cdot (\gamma_T(\lambda) + d_{\mathcal{X}} + \log(T) + H).$$

There exist constants $C_1, C_2 \leq 20$ such that if LC³ (Alg. 1) is run with input parameters λ and C_1 (in Equation 3.3), then following regret bound holds for all T ,

$$\mathbb{E}_{\text{LC}^3} [\text{REGRET}_T] \leq C_2 \tilde{d}_T \sqrt{V_{\max} H T}.$$

While the above regret bound is applicable to the infinite dimensional RKHS setting and does not require uniformly bounded features ϕ , it is informative to specialize the regret bound to the finite dimensional case with bounded features.

Corollary 3.3 (LC³ Regret for finite dimensional, bounded features). *Suppose that Assumptions 1 and 2 hold; d_ϕ is finite; and that ϕ is uniformly bounded, with $\|\phi(x, u)\|_2 \leq B$. Under the same parameter choices as in Theorem 3.2, we have, for all T ,*

$$\mathbb{E}_{\text{LC}^3} [\text{REGRET}_T] \leq C_2 \sqrt{d_\phi (d_\phi + d_\mathcal{X} + \log(T) + H)} V_{\max} H T \cdot \log \left(1 + \frac{B^2 \|W^*\|_2^2 T H}{\sigma^2 d} \right).$$

The above immediately follows from a bound on the finite dimensional information gain (see Lemma C.5).

A few remarks are in order:

Remark 3.4 (Logarithmic parameter dependencies). It is worthwhile noting that our regret bound has only logarithmic dependencies $\|W^*\|_2$ and σ^2 . Furthermore, in the case of finite dimensional and bounded features, the bound is also only logarithmic in the bound B .

Remark 3.5 (Dimension and horizon dependencies). For the special case with bounded $c^t(x, u) \in [0, 1]$, bounded $\phi \in \mathbb{R}^{d_\phi}$, and $d_\phi + d_\mathcal{X} \geq H$, LC³ has a regret bound of $\tilde{O}(\sqrt{d_\phi (d_\phi + d_\mathcal{X}) H^3 T})$. Our dimension dependence matches the lower bounds in [Dani et al., 2008] for linear bandits (where $H = 1$ and $d_\mathcal{X} = 1$). Furthermore, for fixed dimension, one might expect an $\Omega(\sqrt{H^2 T})$ lower bound based on results for tabular MDPs (see Azar et al. [2017], Dann and Brunskill [2015]). Obtaining sharp lower bounds is an important direction for future work.

Remark 3.6 (Linear Quadratic Regulators (LQR) as a special case). Our model generalizes the Linear Quadratic Regulator (LQR). Specifically, we can set $\phi(x, u) = [x^\top, u^\top]^\top$, $c(x, u) = x^\top Q x + u^\top R u$ with Q and R being some PSD matrix. We can consider a policy class to be a (subset) of all linear controls, i.e., $\Pi = \{\pi : u = Kx, K \in \mathcal{K} \subset \mathbb{R}^{d_u \times d_x}\}$.

Consider the case where $d_\mathcal{X} = d_u = d$ (with $d > H$) and the policy class consists of controllable policies (e.g. see Cohen et al. [2019]). Here, our regret scales as $\tilde{O}(\sqrt{H^3 d^4 T})$ (since $V_{\max} = O(Hd^2)$, e.g. see Simchowitz and Foster [2020]). While our rate is a factor of \sqrt{d} larger than the minimax regret bound for an LQR [Simchowitz and Foster, 2020], which is $\Omega(\sqrt{d^3 T})$, our results also apply to non-linear settings, as opposed to the globally linear LQR setting.

The Stabilizing Case, with Bounded Coefficient of Variation

In many cases of practical interest, the optimal cost $J^*(x_0; c)$ may be substantially less than the cost of other controllers, i.e. $J^*(x_0; c) \ll \max_{\pi \in \Pi} J^\pi(x_0; c) < \sqrt{V_{\max}}$. In such cases, one might hope for an improved regret bound for sufficiently large T . We show that this is the case provided our policy class satisfies a certain bounded coefficient of variation condition, which holds for LQRs. Recall the *coefficient of variation* of a random variable is defined as the ratio of the standard deviation to mean.

Assumption 3 (Bounded coefficient of variation at x_0). Assume that the realized cumulative cost, when starting from x_0 , has a uniformly bounded coefficient of variation. Specifically, assume there exists an $\alpha \in \mathbb{R}^+$, such that for every c^t and all $\pi \in \Pi$,

$$\mathbb{E} \left[\left(\sum_{h=0}^{H-1} c^t(x_h, u_h) \right)^2 \middle| x_0, \pi \right] \leq \left(\alpha J^\pi(x_0; c^t) \right)^2.$$

Remark 3.7 (α for LQRs). It is straightforward to verify that Assumption 3 is satisfied in LQRs (with linear controllers) with $\alpha^2 = 3$.

Under this assumption, we can get a regret bound with a leading order term dependent on J^* . The lower order term will depend on a higher moment version of the information gain, defined as follows:

$$\gamma_{2,T}(\lambda) := \max_{\mathcal{A}} \mathbb{E}_{\mathcal{A}} \left[\left(\log \left(\det(\Sigma^{T-1}) / \det(\Sigma^0) \right) \right)^2 \right].$$

Again, for a finite dimensional RKHS with features whose norm bounded is by B , then $\gamma_{2,T}$ will also be $O((d_\phi \log(1 + THB^2/\lambda))^2)$ (see Remark 3.1 and Lemma C.5).

Theorem 3.8 (J^* regret bound). Suppose that Assumptions 1, 2, and 3 hold and that for all t , $J^*(x_0; c^t) \leq J^*$. Again, set $\lambda = \frac{\sigma^2}{\|W^*\|_2^2}$ and define d_T as in Theorem 3.2. There exist absolute constants C_1, C_2 such that if LC^3 (Alg. 1) is run with input parameters C_1 and λ , then the following regret bound holds for all T ,

$$\mathbb{E}_{LC^3} [\text{REGRET}_T] \leq C_2 \left(\alpha J^* \tilde{d}_T \sqrt{HT} + \alpha H \sqrt{V_{\max}} \left(\tilde{d}_T^2 + \gamma_{2,T}(\lambda) \right) \right).$$

See the Discussion (Section 5) for comments on improving the J^* dependence to $\sqrt{J^*}$.

3.3 Proof Techniques

A key technical, “self-bounding” lemma in our proof bounds the difference in cost under two different models, i.e. $J^\pi(x; c, W^*) - J^\pi(x; c, W)$, in terms of the second moment of the cumulative cost itself, i.e. in terms of $V^\pi(x; c, W^*)$, where

$$V^\pi(x; c, W^*) := \mathbb{E} \left[\left(\sum_{h=0}^{H-1} c(x_h, u_h) \right)^2 \middle| x_0 = x, \pi, W^* \right].$$

Lemma 3.9 (Self-Bounding, Simulation Lemma). For any state x , non-negative cost function c , and model W , we have:

$$J^\pi(x; c, W^*) - J^\pi(x; c, W) \leq \sqrt{HV^\pi(x; c, W^*)} \sqrt{\mathbb{E} \left[\sum_{h=0}^{H-1} \min \left\{ \frac{\|(W^* - W) \phi(x_h, u_h)\|_2^2}{\sigma^2}, 1 \right\} \right]}$$

where the expectation is with respect to π in W^* starting at $x_0 = x$.

	InvertedPendulum	Acrobot	CartPole	Mountain Car	Reacher	Hopper
LC ³	-0.0 ± 0.0	95.4 ± 52.5	199.7 ± 0.4	27.3 ± 8.1	-4.1 ± 1.6	-1016.5 ± 607.4
(Ranking)	1/11	1/11	2/11	2/11	1/11	7/11
GT-MPPI	-0.0 ± 0.0	177.8 ± 25.0	199.8 ± 0.1	24.9 ± 2.9	-2.4 ± 0.1	2995.7 ± 215.3
PETS-CEM	-20.5 ± 28.9	12.5 ± 29.0	199.5 ± 3.0	-57.9 ± 3.6	-12.3 ± 5.2	1125.0 ± 679.6
PILCO	-194.5 ± 0.8	-394.4 ± 1.4	-1.9 ± 155.9	-59.0 ± 4.6	-13.2 ± 5.9	-1729.9 ± 1611.1

Table 1: Final performances for six Gym environments. Algorithms are run under the same conditions of Wang et al. [2019]. The performances of PETS-CEM and PILCO are copied for reference, and the performance of ground-truth MPPI (GT-MPPI) that has access to the true model are also shown. The results are averaged over four random seeds and a window size of 5,000 timesteps.

The proof, provided in Appendix B, involves the construction of a certain stopping time martingale to handle the unbounded nature of the (realized) cumulative costs, along with a novel way to handle Gaussian smoothing through the chi-squared distance function between two distributions. This lemma helps us in constructing a potential function for the analysis of the LC³ algorithm.

4 Experiments

We evaluate LC³ on three domains: a set of continuous control tasks, a maze environment that requires exploration, and a dexterous manipulation task. Throughout these experiments, we use model predictive path integral control (MPPI) [Williams et al., 2017] for planning, and posterior reshaping [Chapelle and Li, 2011] (i.e., scaling of posterior covariance) for Thompson sampling – we don’t implement LC³ as analyzed, but rather implement a Thompson sampling variation. The algorithms are implemented in the Lyceum framework under the Julia programming language [Summers et al., 2020, Bezanson et al., 2017]. Comparison algorithms provided by Wang and Ba [2019], Wang et al. [2019]. Note that these experiments use reward (negative cost) for evaluations. Further details of the experiments in this section can be found in Appendix D.

4.1 Benchmark Tasks with Random Features

We use some common benchmark tasks, including MuJoCo [Todorov et al., 2012] environments from OpenAI Gym [Brockman et al., 2016]. We use Random Fourier Features (RFF) [Rahimi and Recht, 2008] to represent ϕ . Fig. 1 plots the learning curves against GT-MPPI and the best model-based RL (MBRL) algorithm reported in Wang et al. [2019]. It is observed that LC³ with RFFs quickly increased reward in early stages, indicating low sample complexities empirically. Table 1 shows the final performances (at 200k timesteps) of LC³ with RFFs for six environments, and includes its ranking compared to the benchmarks results from Wang et al. [2019]. We find that LC³ consistently performs well on simple continuous control tasks, and it works well even without posterior sampling. However, when the dynamical complexity increases, such as with the contact-rich Hopper model, our method’s performance suffers due to non-adaptation of the RFFs. This suggests that more interesting scenarios require different feature representation.

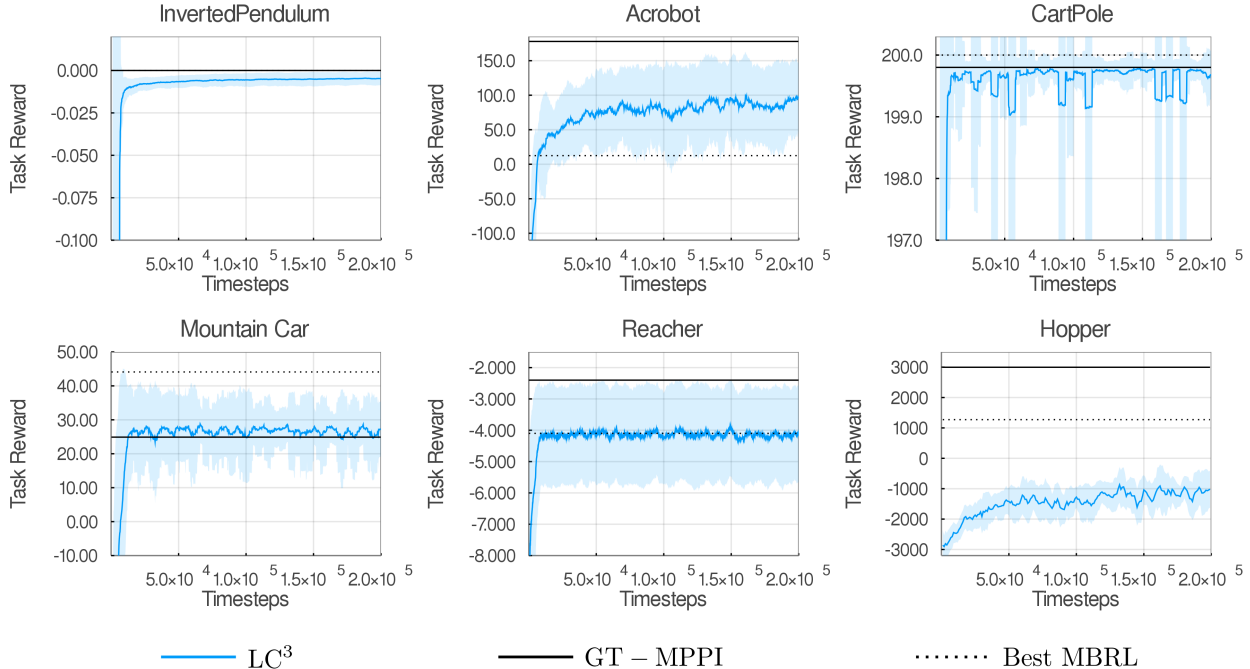


Figure 1: Performance curves of LC^3 with RFFs for different Gym environments. Note the reward (negative cost) ranges of those plots are made different. The final mean performances of GT-MPPI and the best model-based RL (MBRL) algorithm reported in Wang et al. [2019] are also shown for reference. The algorithm is run for 200,000 timesteps and with four random seeds. The curves are averaged over the four random seeds and a window size of 5,000 timesteps.

4.2 Exploring the Maze

We construct a maze environment to study the exploration capability of LC^3 (see Fig. 2 (a)). State and control take values in $[-1, 1]^2 \subset \mathbb{R}^2$ and in $[-1, 1] \subset \mathbb{R}$, respectively. The task is to bring an agent to the goal state being guided by the negative cost (reward) $-c(x_h, u_h) = 8 - \|x_h - [1, 1]^T\|_2^2$. We use a one-hot vector of states and actions as features.

We compare the performances, over 50 episodes with task trajectory length 30, of LC^3 (with different scale parameters for posterior reshaping) to random walk and PETS-CEM. Fig. 2 (b) plots the means and standard deviations, across four random seeds, of the number of state-action pairs visited over episodes. We observe that LC^3 's strategic exploration better modeled the setting for higher rate of success.

4.3 Practical Application

As we might consider learning model dynamics for the real world in applications such as robotics, we need sufficiently complex features – without resorting to large scale data collection for feature learning. One solution to this problem is creating an ensemble of parametric models, such as found

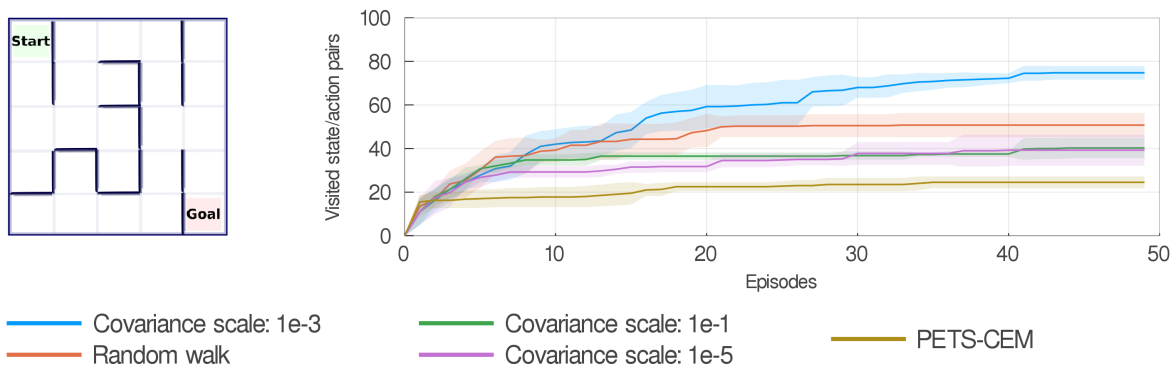


Figure 2: Left: An illustration of the maze environment. Start and End states are $[-1, -1]^T$ and $[1, 1]^T$, respectively. Dark lines are “walls”. Right: The means and standard deviations, across four random seeds, of the number of state-action pairs already explored over episodes. Covariance scale is the posterior reshaping constant of Thompson sampling. Random walk takes actions uniformly sampled within $[-1, 1]$. PETS-CEM is a representative model-based RL which uses uncertainty of dynamics but without exploration. The agent always reaches the goal within 50 episodes under the best setting of LC^3 and the average number of episodes required for the first success is 25.0, while random walk and PETS-CEM never bring the agent to the goal within 50 episodes.

in [Tobin et al. \[2017\]](#), [Mordatch et al. \[2015\]](#). We take the perspective that most model parameters of a robotic system will be known, such as kinematic lengths, actuator specifications, and inertial configurations. Since we would like robots to operate in the wild, some dynamical properties may be unknown: in this case, the manipulated object’s dynamical properties. Said another way, the robot knows about itself, but only a little about the object.

In this experiment, we demonstrate our model learning algorithm on a robotics inspired, dexterous manipulation task. An arm and hand system (see [Fig. 3](#)) must pick up a spherical object with unknown dynamical properties, and hold it at a target position. The entire system has 33 degrees of freedom, and an optimal trajectory would involve numerous discontinuous contacts; the system dynamics are not well captured by random features and such features are not easily learned. We instead use the predictive output of an ensemble of six MuJoCo models as our features ϕ , each with randomized parameters for the object. Using a single model from the ensemble with the planner is unable to perform the task.

[Fig. 3](#) plots the learning curves of LC^3 with different features. We observe that, within 10 attempts at the task, LC^3 with ensemble features is successful, while the same method with RFF features makes no progress. Additionally, we use LC^3 with the top layers of a neural network – trained on a data set of 30 optimized trajectories with the correct model – as our features. It also makes little progress.

We clarify the setting in which this approach may be relevant as follows. Complex dynamics, such as that in the real world, are difficult to represent with function approximation like neural networks or random features. Rather than collect inordinate amounts of data to mimic the com-

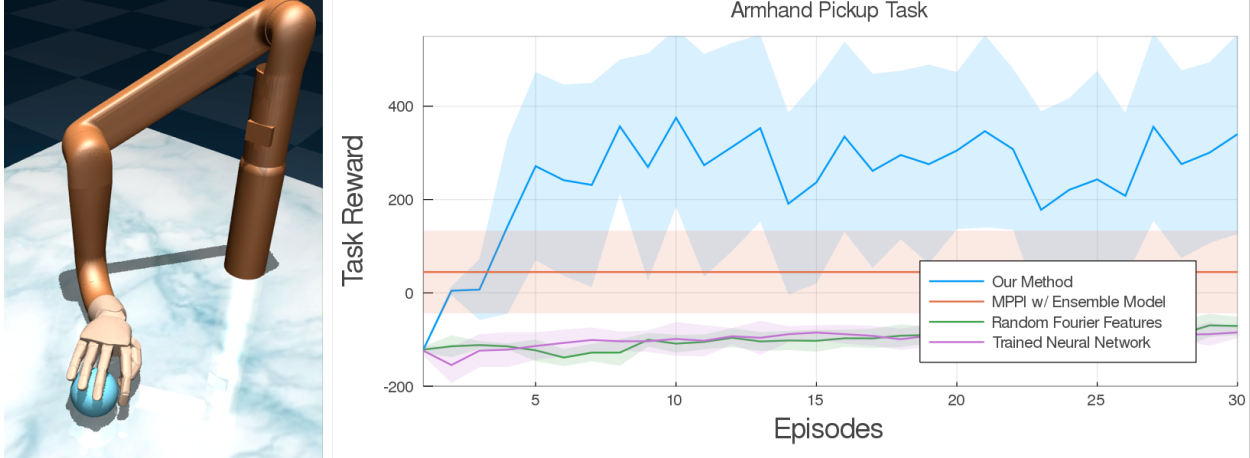


Figure 3: Left: An illustration of Armhand environment. Right: Performance curves averaged across 12 random seeds. For reference, we include the average reward of MPPI using a random model from the ensemble. Its score represents the system moving the hand to the object, but unable to grasp and lift it: exactly what we would expect for randomized object dynamics parameters.

bination of features and model, we instead use structured representations of the real world, such as dynamics simulators, to produce features, and use the method in this work to learn the model. Since dynamics simulators represent the current distillation of physics into a computational form and accurate measurement of engineered systems is paramount for the modern world, this instantiation of this method is reasonable.

5 Discussion

This work provides $O(\sqrt{T})$ regret bounds for the online nonlinear control problem, where we utilize a number of analysis concepts from reinforcement learning and machine learning for continuous problems. Though our work focuses on the theoretical foundations of learning in nonlinear control, we believe our work has broader impact in the following aspects.

Our work helps to further connect two communities: Reinforcement Learning Theory and Control Theory. Existing models considered in RL literature that have provable guarantees rarely are applicable to continuous control problems while only few existing control theory results focus on the (non-asymptotic) sample complexity aspect of controlling unknown dynamical systems. Our work demonstrates that a natural nonlinear control model, the KNR model, is learnable from a learning theoretical perspective.

From a practical application perspective, the sample efficiency of our algorithm enables control in complex dynamical settings without onerous large scale data collection, hence demonstrates potentials for model learning and control in real world applications such as dexterous manipulation, medical robotics, human robot interaction, and self-driving cars where complicated nonlinear dynamics are involved and data is often extremely expensive to collect.

Lastly, there are a number of important extensions and future directions.

Lower bounds: Sharp lower bounds would be important to develop for this very natural model. As discussed in Remark 3.5, our results are already minimax optimal for some parameter scalings.

Improved upper bounds & J^* vs $\sqrt{J^*}$ dependencies: We conjecture with stronger assumptions on higher order moments that an optimal $O(\sqrt{H^2T})$ regret is achievable. It is also plausible that with further higher moment assumptions then, for the stabilizing case, the dependence on J^* can be improved to $\sqrt{J^*}$. Here, our conjecture is that one would, instead, need to make a boundedness assumption on the “index of dispersion,” i.e., that the ratio of the variance to the mean is bounded; we currently assume the ratio of the standard deviation to the mean is bounded.

The single trajectory case: It would be interesting to use these techniques to develop regret bounds for the single trajectory case, under stronger stability and mixing assumptions of the process (see Cohen et al. [2019] for the LQR case).

Feature learning: As of now, we have assumed the RKHS is known. A practically relevant direction would be to learn a good feature space.

Acknowledgments

The authors wish to thank Horia Mania for graciously sharing his thoughts in this line of work. Motoya Ohnishi thanks Aravind Rajeswaran, Vikash Kumar, and Ben Evans at Movement Control Laboratory for valuable discussions on model-based RL. Also, he thanks Colin Summers for instructions on Lyceum. Kendall Lowrey and Motoya Ohnishi thank Emanuel Todorov for valuable discussions and Roboti LLC for computational supports. Sham Kakade acknowledges funding from the Washington Research Foundation for Innovation in Data-intensive Discovery, the ONR award N00014-18-1-2247, NSF Award CCF-1703574, and the NSF Award CCF-1637360. Motoya Ohnishi was supported in part by Wissner-Slivka Endowed Fellowship and Funai Overseas Scholarship.

References

- Yasin Abbasi-Yadkori and Csaba Szepesvári. Regret bounds for the adaptive control of linear quadratic systems. In *Conference on Learning Theory*, pages 1–26, 2011.
- Yasin Abbasi-Yadkori, Dávid Pál, and Csaba Szepesvári. Improved algorithms for linear stochastic bandits. In *Advances in Neural Information Processing Systems*, pages 2312–2320, 2011.
- Pieter Abbeel and Andrew Y Ng. Exploration and apprenticeship learning in reinforcement learning. In *Proceedings of the 22nd international conference on Machine learning*, pages 1–8, 2005.

- Alekh Agarwal, Sham M. Kakade, Jason D. Lee, and Gaurav Mahajan. Optimality and approximation with policy gradient methods in Markov decision processes. *arXiv preprint arXiv:1908.00261*, 2019a.
- Naman Agarwal, Brian Bullins, Elad Hazan, Sham M. Kakade, and Karan Singh. Online control with adversarial disturbances. *arXiv preprint arXiv:1902.08721*, 2019b.
- Naman Agarwal, Elad Hazan, and Karan Singh. Logarithmic regret for online control. In *Advances in Neural Information Processing Systems*, pages 10175–10184, 2019c.
- Hyo-Sung Ahn, YangQuan Chen, and Kevin L. Moore. Iterative learning control: Brief survey and categorization. *IEEE Transactions on Systems, Man, and Cybernetics, Part C (Applications and Reviews)*, 37(6):1099–1121, 2007.
- Ilge Akkaya, Marcin Andrychowicz, Maciek Chociej, Mateusz Litwin, Bob McGrew, Arthur Petron, Alex Paino, Matthias Plappert, Glenn Powell, Raphael Ribas, Jonas Schneider, Nikolas Tezak, Jerry Tworek, Peter Welinder, Lilian Weng, Qiming Yuan, Wojciech Zaremba, and Lei Zhang. Solving rubik’s cube with a robot hand. *arXiv preprint arXiv:1910.07113*, 2019.
- Mazen Al Borno, Martin De Lasa, and Aaron Hertzmann. Trajectory optimization for full-body movements with complex contacts. *IEEE Transactions on Visualization and Computer Graphics*, 19(8):1405–1414, 2012.
- Alex Ayoub, Zeyu Jia, Csaba Szepesvari, Mengdi Wang, and Lin F Yang. Model-based reinforcement learning with value-targeted regression. *arXiv preprint arXiv:2006.01107*, 2020.
- Mohammad Gheshlaghi Azar, Ian Osband, and Rémi Munos. Minimax regret bounds for reinforcement learning. In *International Conference on Machine Learning*, pages 263–272, 2017.
- Marc Bellemare, Sriram Srinivasan, Georg Ostrovski, Tom Schaul, David Saxton, and Remi Munos. Unifying count-based exploration and intrinsic motivation. In *Advances in neural information processing systems*, pages 1471–1479, 2016.
- Jeff Bezanson, Alan Edelman, Stefan Karpinski, and Viral B Shah. Julia: A fresh approach to numerical computing. *SIAM review*, 59(1):65–98, 2017. URL <https://doi.org/10.1137/141000671>.
- Greg Brockman, Vicki Cheung, Ludwig Pettersson, Jonas Schneider, John Schulman, Jie Tang, and Wojciech Zaremba. Openai Gym. *arXiv preprint arXiv:1606.01540*, 2016.
- Yuri Burda, Harrison Edwards, Amos Storkey, and Oleg Klimov. Exploration by random network distillation. *arXiv preprint arXiv:1810.12894*, 2018.
- Olivier Chapelle and Lihong Li. An empirical evaluation of Thompson sampling. In *Advances in Neural Information Processing Systems*, pages 2249–2257, 2011.

- Kurtland Chua, Roberto Calandra, Rowan McAllister, and Sergey Levine. Deep reinforcement learning in a handful of trials using probabilistic dynamics models. In *Advances in Neural Information Processing Systems*, pages 4754–4765, 2018.
- Alon Cohen, Avinatan Hassidim, Tomer Koren, Nevena Lazic, Yishay Mansour, and Kunal Talwar. Online linear quadratic control. In *International Conference on Machine Learning*, pages 1029–1038, 2018.
- Alon Cohen, Tomer Koren, and Yishay Mansour. Learning linear-quadratic regulators efficiently with only \sqrt{T} regret. In *International Conference on Machine Learning*, pages 1300–1309, 2019.
- Varsha Dani, Thomas P. Hayes, and Sham M. Kakade. Stochastic linear optimization under bandit feedback. In *Conference on Learning Theory*, pages 355–366, 2008.
- Christoph Dann and Emma Brunskill. Sample complexity of episodic fixed-horizon reinforcement learning. In *Advances in Neural Information Processing Systems*, pages 2818–2826, 2015.
- Sarah Dean, Horia Mania, Nikolai Matni, Benjamin Recht, and Stephen Tu. Regret bounds for robust adaptive control of the linear quadratic regulator. In *Advances in Neural Information Processing Systems*, pages 4188–4197, 2018.
- Marc Deisenroth and Carl E. Rasmussen. PILCO: A model-based and data-efficient approach to policy search. In *International Conference on Machine Learning*, pages 465–472, 2011.
- Elad Hazan, Sham M. Kakade, and Karan Singh. The nonstochastic control problem. *arXiv preprint arXiv:1911.12178*, 2019.
- David H. Jacobson and David Q. Mayne. *Differential dynamic programming*. American Elsevier Pub. Co., 1970.
- Nan Jiang, Akshay Krishnamurthy, Alekh Agarwal, John Langford, and Robert E. Schapire. Contextual decision processes with low Bellman rank are PAC-learnable. In *International Conference on Machine Learning*, pages 1704–1713, 2017.
- Sham M. Kakade. *On the sample complexity of reinforcement learning*. PhD thesis, Gatsby Computational Neuroscience Unit, University College, London, 2003.
- Sham M. Kakade, Michael J. Kearns, and John Langford. Exploration in metric state spaces. In *International Conference on Machine Learning*, pages 306–312, 2003.
- Michael Kearns and Satinder Singh. Near-optimal reinforcement learning in polynomial time. *Machine learning*, 49(2-3):209–232, 2002.
- V. Kumar, E. Todorov, and S. Levine. Optimal control with learned local models: Application to dexterous manipulation. In *IEEE International Conference on Robotics and Automation*, pages 378–383, 2016.

- Thanard Kurutach, Ignasi Clavera, Yan Duan, Aviv Tamar, and Pieter Abbeel. Model-ensemble trust-region policy optimization. *arXiv preprint arXiv:1802.10592*, 2018.
- Sergey Levine and Pieter Abbeel. Learning neural network policies with guided policy search under unknown dynamics. In *Advances in Neural Information Processing Systems*, pages 1071–1079, 2014.
- Kendall Lowrey, Aravind Rajeswaran, Sham M. Kakade, Emanuel Todorov, and Igor Mordatch. Plan online, learn offline: Efficient learning and exploration via model-based control. *arXiv preprint arXiv:1811.01848*, 2018.
- Xiuyuan Lu and Benjamin Van Roy. Information-theoretic confidence bounds for reinforcement learning. In *Advances in Neural Information Processing Systems*, pages 2458–2466, 2019.
- Yuping Luo, Huazhe Xu, Yuanzhi Li, Yuandong Tian, Trevor Darrell, and Tengyu Ma. Algorithmic framework for model-based deep reinforcement learning with theoretical guarantees. *arXiv preprint arXiv:1807.03858*, 2018.
- Horia Mania, Stephen Tu, and Benjamin Recht. Certainty equivalent control of LQR is efficient. *arXiv preprint arXiv:1902.07826*, 2019.
- Horia Mania, Michael I. Jordan, and Benjamin Recht. Active learning for nonlinear system identification with guarantees. *arXiv preprint arXiv:2006.10277*, 2020.
- Igor Mordatch, Emanuel Todorov, and Zoran Popović. Discovery of complex behaviors through contact-invariant optimization. *ACM Transactions on Graphics*, 31(4):1–8, 2012.
- Igor Mordatch, Kendall Lowrey, and Emanuel Todorov. Ensemble-CIO: Full-body dynamic motion planning that transfers to physical humanoids. In *IEEE International Conference on Intelligent Robots and Systems*, pages 5307–5314, 2015.
- Anusha Nagabandi, Gregory Kahn, Ronald S. Fearing, and Sergey Levine. Neural network dynamics for model-based deep reinforcement learning with model-free fine-tuning. In *IEEE International Conference on Robotics and Automation*, pages 7559–7566, 2018.
- Andrew Y Ng, Adam Coates, Mark Diel, Varun Ganapathi, Jamie Schulte, Ben Tse, Eric Berger, and Eric Liang. Autonomous inverted helicopter flight via reinforcement learning. In *Experimental robotics IX*, pages 363–372. Springer, 2006.
- Ian Osband and Benjamin Van Roy. Model-based reinforcement learning and the Eluder dimension. In *Advances in Neural Information Processing Systems*, pages 1466–1474, 2014.
- Deepak Pathak, Pulkit Agrawal, Alexei A. Efros, and Trevor Darrell. Curiosity-driven exploration by self-supervised prediction. In *International Conference on Machine Learning*, pages 16–17, 2017.

- Alejandro Perez, Robert Platt, George Konidaris, Leslie Kaelbling, and Tomas Lozano-Perez. LQR-RRT*: Optimal sampling-based motion planning with automatically derived extension heuristics. In *IEEE International Conference on Robotics and Automation*, pages 2537–2542, 2012.
- Ali Rahimi and Benjamin Recht. Random features for large-scale kernel machines. In *Advances in Neural Information Processing Systems*, pages 1177–1184, 2008.
- Stephane Ross and J. Andrew Bagnell. Agnostic system identification for model-based reinforcement learning. In *International Conference on Machine Learning*, pages 190–1912, 2012.
- Daniel Russo and Benjamin Van Roy. Eluder dimension and the sample complexity of optimistic exploration. In *Advances in Neural Information Processing Systems*, pages 2256–2264, 2013.
- Daniel Russo and Benjamin Van Roy. Learning to optimize via posterior sampling. *Mathematics of Operations Research*, 39(4):1221–1243, 2014.
- Shai Shalev-Shwartz and Shai Ben-David. *Understanding machine learning: From theory to algorithms*. Cambridge university press, 2014.
- David Silver, Aja Huang, Chris J. Maddison, Arthur Guez, Laurent Sifre, George van den Driessche, Julian Schrittwieser, Ioannis Antonoglou, Veda Panneershelvam, Marc Lanctot, Sander Dieleman, Dominik Grewe, John Nham, Nal Kalchbrenner, Ilya Sutskever, Timothy Lillicrap, Madeleine Leach, Koray Kavukcuoglu, Thore Graepel, and Demis Hassabis. Mastering the game of Go with deep neural networks and tree search. *Nature*, 529:484–489, 2016.
- Max Simchowitz and Dylan J Foster. Naive exploration is optimal for online LQR. *arXiv preprint arXiv:2001.09576*, 2020.
- Niranjan Srinivas, Andreas Krause, Sham M. Kakade, and Matthias Seeger. Gaussian process optimization in the bandit setting: No regret and experimental design. *arXiv preprint arXiv:0912.3995*, 2009.
- Colin Summers, Kendall Lowrey, Aravind Rajeswaran, Siddhartha Srinivasa, and Emanuel Todorov. Lyceum: An efficient and scalable ecosystem for robot learning. *arXiv preprint arXiv:2001.07343*, 2020.
- Wen Sun, Nan Jiang, Akshay Krishnamurthy, Alekh Agarwal, and John Langford. Model-based RL in contextual decision processes: PAC bounds and exponential improvements over model-free approaches. In *Conference on Learning Theory*, pages 1–36, 2019.
- Russ Tedrake. LQR-trees: Feedback motion planning on sparse randomized trees. 2009.
- William R. Thompson. On the likelihood that one unknown probability exceeds another in view of the evidence of two samples. *Biometrika*, 25(3/4):285–294, 1933.

- Josh Tobin, Rachel Fong, Alex Ray, Jonas Schneider, Wojciech Zaremba, and Pieter Abbeel. Domain randomization for transferring deep neural networks from simulation to the real world. In *IEEE International Conference on Intelligent Robots and Systems*, pages 23–30, 2017.
- Emanuel Todorov and Weiwei Li. A generalized iterative LQG method for locally-optimal feedback control of constrained nonlinear stochastic systems. In *American Control Conference*, pages 300–306, 2005.
- Emanuel Todorov, Tom Erez, and Yuval Tassa. MuJoCo: A physics engine for model-based control. In *IEEE International Conference on Intelligent Robots and Systems*, pages 5026–5033, 2012.
- Nolan Wagener, Ching-An Cheng, Jacob Sacks, and Byron Boots. An online learning approach to model predictive control. In *Robotics: Science and Systems*, 2019.
- Tingwu Wang and Jimmy Ba. Exploring model-based planning with policy networks. *arXiv preprint arXiv:1906.08649*, 2019.
- Tingwu Wang, Xuchan Bao, Ignasi Clavera, Jerrick Hoang, Yeming Wen, Eric Langlois, Shunshi Zhang, Guodong Zhang, Pieter Abbeel, and Jimmy Ba. Benchmarking model-based reinforcement learning. *arXiv preprint arXiv:1907.02057*, 2019.
- Grady Williams, Andrew Aldrich, and Evangelos A. Theodorou. Model predictive path integral control: From theory to parallel computation. *Journal of Guidance, Control, and Dynamics*, 40(2):344–357, 2017.

A Additional Notation

A controller is a mapping $\pi : \mathcal{X} \times \{0, \dots, H - 1\} \rightarrow \mathcal{U}$. Given a instantaneous cost function $c : \mathcal{X} \times \mathcal{U} \rightarrow \mathbb{R}$, we define the cost (or the ‘‘cost-to-go’’) of a policy as:

$$J^\pi(x; c, W) = \mathbb{E} \left[\sum_{h=0}^{H-1} c(x_h, u_h) \middle| \pi, x_0 = x, W \right]$$

where the expectation is under trajectories sampled under π starting from x_0 in model parameterized by W . The ‘‘cost-to-go’’ at state x at time $h \in \{0, \dots, H - 1\}$ is denoted by:

$$J_h^\pi(x; c, W) = \mathbb{E} \left[\sum_{\ell=h}^{H-1} c(x_\ell, u_\ell) \middle| \pi, x_h = x \right].$$

When clear from context, we let the episode t index the policy, e.g. we write $J^t(x; c)$ to refer to $J^{\pi^t}(x, c)$. Subscripts refer to the timestep within an episode and superscripts index the episode itself, i.e. ϕ_h^t will refer to the random vector which is the observed features during timestep h within episode t . We let \mathcal{H}_t denote the history up to the beginning of episode t .

Also, $\|x\|_M^2 := x^\top M x$ for a vector x and a matrix M .

B Lower Confidence Bound based Analysis

In this section, we provide proofs for the two main theorems: Theorem 3.2 and Theorem 3.8.

B.1 Simulation Analysis

We derive a novel self-bounding simulation lemma (Lemma B.3) in this section, using the Optional Stopping Theorem.

Lemma B.1 (Difference Lemma). *Fix a policy π , cost function c , and model W . Consider any trajectory $\{x_h, u_h\}_{h=0}^{H-1}$ where $u_h = \pi(x_h)$ for all $h \in \{0, \dots, H - 1\}$. For $h \in \{0, \dots, H - 1\}$, let \widehat{J}_h refer to the realized cost-to-go on this trajectory, i.e.*

$$\widehat{J}_h = \sum_{\tau=h}^{H-1} c(x_\tau, u_\tau).$$

For all $\tau \in \{1, \dots, H - 1\}$, we have that:

$$\begin{aligned} \widehat{J}_0 - J_0^\pi(x_0; c, W) &= \widehat{J}_\tau - \mathbb{E}_{x'_\tau \sim P(\cdot | W, x_{\tau-1}, u_{\tau-1})} J_\tau^\pi(x'_\tau; c, W) \\ &\quad + \sum_{h=1}^{\tau-1} J_h^\pi(x_h; c, W) - \mathbb{E}_{x'_h \sim P(\cdot | W, x_{h-1}, u_{h-1})} J_h^\pi(x'_h; c, W) \end{aligned}$$

Proof. Starting from $h = 0$, using $u_0 = \pi(x_0)$, we have:

$$\begin{aligned}
\widehat{J}_0 - J_0^\pi(x_0; c, W) &= \widehat{J}_1 - \mathbb{E}_{x'_1 \sim P(\cdot | W, x_0, u_0)} J_1^\pi(x'_1; c, W) \\
&= \widehat{J}_1 - J_1^\pi(x_1; c, W) + J_1^\pi(x_1; c, W) - \mathbb{E}_{x'_1 \sim P(\cdot | W, x_0, u_0)} J_1^\pi(x'_1; c, W) \\
&= \widehat{J}_2 - \mathbb{E}_{x'_2 \sim P(\cdot | x_1, u_1, W)} J_2^\pi(x'_2; c, W) \\
&\quad + J_1^\pi(x_1; c, W) - \mathbb{E}_{x'_1 \sim P(\cdot | W, x_0, u_0)} J_1^\pi(x'_1; c, W).
\end{aligned}$$

Recursion completes the proof, where, at each step of the recursion, we add and subtract $J_t^\pi(x_t; c, W)$ and apply the same operation on the term $\widehat{J}_t - J_t^\pi(x_t; c, W)$; \square

Lemma B.2 (“Optional Stopping” Simulation Lemma). *Fix a policy π , cost function c , and model W . Consider the stochastic process over trajectories, where $\{x_h, u_h\}_{h=0}^H \sim \pi$ is sampled with respect to the model W^* . With respect to this stochastic process, define a stopping time τ as:*

$$\tau = \min \{h \geq 0 : J_h^\pi(x_h; c, W) \geq J_h^\pi(x_h; c, W^*)\}.$$

Define the random variable $\widetilde{J}_h^\pi(x_h)$ as:

$$\widetilde{J}_h^\pi(x_h) = \min \{J_h^\pi(x_h; c, W), J_h^\pi(x_h; c, W^*)\}.$$

We have that:

$$\begin{aligned}
&J_0^\pi(x_0; c, W^*) - J_0^\pi(x_0; c, W) \\
&\leq \mathbb{E} \left[\sum_{h=0}^{H-1} 1\{h < \tau\} \left(\mathbb{E}_{x'_{h+1} \sim P(\cdot | W^*, x_h, u_h)} \widetilde{J}_{h+1}^\pi(x'_{h+1}) - \mathbb{E}_{x'_{h+1} \sim P(\cdot | W, x_h, u_h)} \widetilde{J}_{h+1}^\pi(x'_{h+1}) \right) \right]
\end{aligned}$$

where the expectation is with respect to $\{x_h, u_h\}_{h=0}^H \sim \pi$ sampled with respect to the model W^* .

Proof. Our filtration, \mathcal{F}_h , at time h will be the previous noise variables, i.e.

$$\mathcal{F}_h := \{\epsilon_0, \epsilon_1 \dots \epsilon_{h-1}\},$$

and note that $\{x_1, u_1, c(x_1, u_1), \dots, x_h, u_h, c(x_h, u_h)\}$ is fully determined by \mathcal{F}_h . Also, observe that τ is a valid stopping time with respect to the filtration \mathcal{F}_h .

Define:

$$M_h = \mathbb{E} \left[\widehat{J}_0 - J^*(x_0; c, W) \mid \mathcal{F}_h \right]$$

which is a Doob martingale (with respect to our filtration), and so $\mathbb{E}[M_{h+1} | \mathcal{F}_h] = M_h$. By Doob’s optional stopping theorem,

$$\mathbb{E} \left[\widehat{J}_0 - J^*(x_0; c, W) \right] = \mathbb{E}[M_\tau] = \mathbb{E} \left[\mathbb{E} \left[\widehat{J}_0 - J^*(x_0; c, W) \mid \mathcal{F}_\tau \right] \right]. \quad (\text{B.1})$$

The proof consists in bounding M_τ .

Consider an \mathcal{F}_τ , which is stopped at the random time τ . By Lemma B.1,

$$\begin{aligned}
M_\tau &= \mathbb{E} \left[\widehat{J}_0 - J^*(x_0; c, W) \mid \mathcal{F}_\tau \right] \\
&= J_\tau(x_\tau; c, W^*) - \mathbb{E}_{x'_\tau \sim P(\cdot | W, x_{\tau-1}, u_{\tau-1})} J_h(x'_\tau; c, W) \\
&\quad + \sum_{h=1}^{\tau-1} \left(J_h(x_h; c, W) - \mathbb{E}_{x'_h \sim P(\cdot | W, x_{h-1}, u_{h-1})} J_h(x'_h; c, W) \right) \\
&= \sum_{h=1}^{\tau} \left(\widetilde{J}_h(x_h) - \mathbb{E}_{x'_h \sim P(\cdot | W, x_{h-1}, u_{h-1})} J_h(x'_h; c, W) \right) \\
&\leq \sum_{h=1}^{\tau} \left(\widetilde{J}_h(x_h) - \mathbb{E}_{x'_h \sim P(\cdot | W, x_{h-1}, u_{h-1})} \widetilde{J}_h(x'_h) \right) \\
&= \sum_{h=1}^H \mathbf{1}(h \leq \tau) \left(\widetilde{J}_h(x_h) - \mathbb{E}_{x'_h \sim P(\cdot | W, x_{h-1}, u_{h-1})} \widetilde{J}_h(x'_h) \right).
\end{aligned}$$

where the third equality follows using the definition of τ which implies that $J_\tau(x_\tau; c, W^*) = \widetilde{J}_\tau(x_\tau)$ and that $J_h(x_h; c, W) = \widetilde{J}_h(x_h)$ for $h < \tau$; and the inequality is due to the definition of \widetilde{J} .

Using this bound on M_τ and Equation B.1, we have:

$$\mathbb{E} \left[\widehat{J}_0 - J^*(x_0; c, W) \right] \leq \sum_{h=1}^H \mathbb{E} \left[\mathbf{1}(h \leq \tau) \left(\widetilde{J}_h(x_h) - \mathbb{E}_{x'_h \sim P(\cdot | W, x_{h-1}, u_{h-1})} \widetilde{J}_h(x'_h) \right) \right].$$

For the h -th term, observe:

$$\begin{aligned}
&\mathbb{E} \left[\mathbf{1}(h \leq \tau) \left(\widetilde{J}_h(x_h) - \mathbb{E}_{x'_h \sim P(\cdot | W, x_{h-1}, u_{h-1})} \widetilde{J}_h(x'_h) \right) \right] \\
&= \mathbb{E} \left[\mathbb{E} \left[\mathbf{1}(h \leq \tau) \left(\widetilde{J}_h(x_h) - \mathbb{E}_{x'_h \sim P(\cdot | W, x_{h-1}, u_{h-1})} \widetilde{J}_h(x'_h) \right) \mid \mathcal{F}_{h-1} \right] \right] \\
&= \mathbb{E} \left[\mathbb{E} \left[\mathbf{1}(h-1 < \tau) \left(\widetilde{J}_h(x_h) - \mathbb{E}_{x'_h \sim P(\cdot | W, x_{h-1}, u_{h-1})} \widetilde{J}_h(x'_h) \right) \mid \mathcal{F}_{h-1} \right] \right] \\
&= \mathbb{E} \left[\mathbf{1}(h-1 < \tau) \mathbb{E} \left[\widetilde{J}_h(x_h) - \mathbb{E}_{x'_h \sim P(\cdot | W, x_{h-1}, u_{h-1})} \widetilde{J}_h(x'_h) \mid \mathcal{F}_{h-1} \right] \right] \\
&= \mathbb{E} \left[\mathbf{1}(h-1 < \tau) \left(\mathbb{E}_{x'_h \sim P(\cdot | W^*, x_{h-1}, u_{h-1})} \widetilde{J}_h(x'_h) - \mathbb{E}_{x'_h \sim P(\cdot | W, x_{h-1}, u_{h-1})} \widetilde{J}_h(x'_h) \right) \right].
\end{aligned}$$

where the second equality uses that $\mathbf{1}(h \leq \tau) = \mathbf{1}(h-1 < \tau)$, and the third equality uses that $\mathbf{1}(h-1 < \tau)$ is measurable with respect to $\mathcal{F}_{h-1} = \{\epsilon_0, \dots, \epsilon_{h-2}\}$. This completes the proof. \square

The previous lemma allows us to bound the difference in cost under two different models, i.e. $J^\pi(x; c, W^*) - J^\pi(x; c, W)$, in terms of the second moment of the cumulative cost itself, i.e. in terms of $V^\pi(x; c, W^*)$, where

$$V^\pi(x_0; c, W^*) := \mathbb{E} \left[\left(\sum_{h=0}^{H-1} c(x_h, u_h) \right)^2 \mid x_0, \pi, W^* \right].$$

Lemma B.3 (Self-Bounding, Simulation Lemma). *For any policy π , model parameterization W , and non-negative cost c , and for any state x_0 , we have:*

$$\begin{aligned} & J^\pi(x_0; c, W^*) - J^\pi(x_0; c, W) \\ & \leq \sqrt{HV^\pi(x_0; c, W^*)} \sqrt{\mathbb{E} \left[\sum_{h=0}^{H-1} \min \left\{ \frac{1}{\sigma^2} \|(W^* - W) \phi(x_h, u_h)\|_2^2, 1 \right\} \right]}. \end{aligned}$$

where the expectation is with respect to π in W^* starting at x_0 .

Proof. For the proof, it is helpful to define the random variables:

$$\begin{aligned} \Delta_h &= \mathbb{E}_{x'_{h+1} \sim P(\cdot | W^*, x_h, u_h)} \left[\tilde{J}_{h+1}(x'_{h+1}) \right] - \mathbb{E}_{x'_{h+1} \sim P(\cdot | W, x_h, u_h)} \left[\tilde{J}_{h+1}(x'_{h+1}) \right] \\ A_h &:= \mathbb{E}_{x'_{h+1} \sim P(\cdot | W^*, x_h, u_h)} \left[\tilde{J}_{h+1}(x'_{h+1})^2 \right] \end{aligned}$$

By Lemma C.2 (which bounds the difference in means under two Gaussian distributions, using the chi-squared distance function), we have:

$$\begin{aligned} \Delta_h &\leq \sqrt{\mathbb{E}_{x_{h+1} \sim P(\cdot | W^*, x_h, u_h)} \left[\tilde{J}_{h+1}(x_{h+1})^2 \right]} \min \left\{ \frac{1}{\sigma} \|(W^* - W) \phi(x_h, u_h)\|_2, 1 \right\} \\ &= \sqrt{A_h} \min \left\{ \frac{1}{\sigma} \|(W^* - W) \phi(x_h, u_h)\|_2, 1 \right\}. \end{aligned}$$

From Lemma B.2, we have:

$$\begin{aligned} & J_0^\pi(x_0; c, W^*) - J_0^\pi(x_0; c, W) \leq \sum_{h=0}^{H-1} \mathbb{E} [1(h < \tau) \Delta_h] \\ & \leq \sum_{h=0}^{H-1} \mathbb{E} \left[\sqrt{A_h} \min \left\{ \frac{1}{\sigma} \|(W^* - W) \phi(x_h, u_h)\|_2, 1 \right\} \right] \\ & \leq \sum_{h=0}^{H-1} \sqrt{\mathbb{E} [A_h]} \sqrt{\mathbb{E} \left[\min \left\{ \frac{1}{\sigma^2} \|(W^* - W) \phi(x_h, u_h)\|_2^2, 1 \right\} \right]} \\ & \leq \sqrt{\mathbb{E} \left[\sum_{h=0}^{H-1} A_h \right]} \sqrt{\mathbb{E} \left[\sum_{h=0}^{H-1} \min \left\{ \frac{1}{\sigma^2} \|(W^* - W) \phi(x_h, u_h)\|_2^2, 1 \right\} \right]}, \end{aligned}$$

where in the second inequality we use $\mathbb{E}[ab] \leq \sqrt{\mathbb{E}[a^2]\mathbb{E}[b^2]}$ and the Cauchy-Schwartz inequality

in the last inequality. For the first term, observe that:

$$\begin{aligned}
\mathbb{E}[A_h] &= \mathbb{E} \left[\mathbb{E}_{x'_{h+1} \sim P(\cdot | W^*, x_h, u_h)} \left[\tilde{J}_{h+1}(x'_{h+1})^2 \right] \right] = \mathbb{E} \left[\tilde{J}_{h+1}(x_{h+1})^2 \right] \leq \mathbb{E} \left[J_{h+1}(x_{h+1})^2 \right] \\
&= \mathbb{E} \left[\left(\mathbb{E} \left[\sum_{\ell=h+1}^{H-1} c(x_\ell, u_\ell) \mid x_{h+1} \right] \right)^2 \right] \leq \mathbb{E} \left[\left(\sum_{\ell=h+1}^{H-1} c(x_\ell, u_\ell) \right)^2 \right] \\
&\leq \mathbb{E} \left[\left(\sum_{\ell=0}^{H-1} c(x_\ell, u_\ell) \right)^2 \right] = V^\pi
\end{aligned}$$

where the first inequality uses the definition of \tilde{J} ; the second inequality follows from Jensen's inequality; and the last inequality follows from our assumption that the instantaneous costs are non-negative. The proof is completed by substitution. \square

B.2 Regret Analysis (and proofs of Theorem 3.2 and Theorem 3.8)

Throughout, let $\mathcal{E}_{t,cb}$ be the event that $W^* \in \text{BALL}^t$ holds at episode t .

Lemma B.4 (Per-episode Regret Lemma). *Suppose Assumptions 1 and 2 hold. Let $\mathcal{H}_{<t}$ be the history of events before episode t . For the LC^3 , we have:*

$$\begin{aligned}
&\mathbf{1}(\mathcal{E}_{t,cb}) \left(J^t(x_0; c^t) - J^*(x_0; c^t) \right) \\
&\leq \sqrt{HV^t(x_0; c, W^*) \left(\frac{4\beta^t}{\sigma^2} + H \right)} \sqrt{\mathbb{E} \left[\min \left\{ \sum_{h=0}^{H-1} \|\phi_h^t\|_{(\Sigma^t)^{-1}}^2, 1 \right\} \mid \mathcal{H}_{<t} \right]}.
\end{aligned}$$

Note that the expectation is with respect to the trajectory of LC^3 , i.e. it is under π^t in W^* .

Proof. Suppose \mathcal{E}_{cb}^t holds, else the lemma is immediate. By construction of the LC^3 algorithm (the optimistic property) and by the self-bounding, simulation lemma (Lemma B.3), we have:

$$\begin{aligned}
&J^t(x_0; c^t, W^*) - J^*(x_0; c^t, W^*) \leq J^t(x_0; c^t, W^*) - J^t(x_0; c^t, \widehat{W}^t) \\
&\leq \sqrt{HV^t(x_0; c, W^*)} \sqrt{\mathbb{E} \left[\sum_{h=0}^{H-1} \min \left\{ \frac{1}{\sigma^2} \left\| (W^* - \widehat{W}^t) \phi_h^t \right\|_2^2, 1 \right\} \mid \mathcal{H}_{<t} \right]}.
\end{aligned}$$

where the expectation is with respect to the trajectory of LC^3 , i.e. of π^t in W^* .

For $W^* \in \text{BALL}^t$, we have

$$\begin{aligned}
&\left\| (\widehat{W}^t - W^*) \phi_h^t \right\|_2 \leq \left\| (\widehat{W}^t - W^*) (\Sigma^t)^{1/2} \right\|_2 \left\| (\Sigma^t)^{-1/2} \phi_h^t \right\|_2 \\
&\leq \left(\left\| (\widehat{W}^t - \overline{W}^t) (\Sigma^t)^{1/2} \right\|_2 + \left\| (\overline{W}^t - W^*) (\Sigma^t)^{1/2} \right\|_2 \right) \left\| \phi_h^t \right\|_{(\Sigma^t)^{-1}} \leq 2\sqrt{\beta^t} \left\| \phi_h^t \right\|_{(\Sigma^t)^{-1}}.
\end{aligned}$$

where we have also used that $\widehat{W}^t, \overline{W}^t \in \text{BALL}^t$, by construction.

This implies that:

$$\begin{aligned} \sum_{h=0}^{H-1} \min \left\{ \frac{1}{\sigma^2} \|(W^* - \widehat{W}^t)\phi_h^t\|_2^2, 1 \right\} &\leq \sum_{h=0}^{H-1} \min \left\{ \frac{4\beta^t}{\sigma^2} \|\phi_h^t\|_{(\Sigma^t)^{-1}}^2, 1 \right\} \\ &\leq \min \left\{ \frac{4\beta^t}{\sigma^2} \sum_{h=0}^{H-1} \|\phi_h^t\|_{(\Sigma^t)^{-1}}^2, H \right\} \leq \max \left\{ \frac{4\beta^t}{\sigma^2}, H \right\} \min \left\{ \sum_{h=0}^{H-1} \|\phi_h^t\|_{(\Sigma^t)^{-1}}^2, 1 \right\}. \end{aligned}$$

The proof is completed by substitution. \square

Before we complete the proofs, the following two lemmas are helpful. Their proofs are provided in Appendix B.3. The first lemma bounds the sum failure probability of W^* not being in all the confidence balls (over all the episodes); the lemma generalizes the argument from [Abbasi-Yadkori et al., 2011, Dani et al., 2008] to matrix regression.

Lemma B.5 (Confidence Ball). *Let*

$$\beta^t = 2\lambda \|W^*\|_2^2 + 8\sigma^2 (d_{\mathcal{X}} \log(5) + 2 \log(t) + \log(4) + \log(\det(\Sigma^t)/\det(\Sigma^0))).$$

We have:

$$\sum_{t=0}^{\infty} \Pr(\mathcal{E}_{t,cb}) = \sum_{t=0}^{\infty} \Pr\left(\left\|(\overline{W}^t - W^*) (\Sigma^t)^{1/2}\right\|_2^2 > \beta^t\right) \leq \frac{1}{2}.$$

The next lemma provides a bound on the potential function used in our analysis. It is based on the elliptical potential function argument from [Dani et al., 2008, Srinivas et al., 2009].

Lemma B.6 (Sum of Potential Functions). *For any sequence of ϕ_h^t , we have:*

$$\sum_{t=0}^{T-1} \min \left\{ \sum_{h=0}^{H-1} \|\phi_h^t\|_{(\Sigma^t)^{-1}}^2, 1 \right\} \leq 2 \log(\det(\Sigma^T) \det(\Sigma^0)^{-1}).$$

Also, recall that LC³ uses the setting of $\lambda = \sigma^2/\|W^*\|_2^2$. We will also use that, for β^T as defined in Lemma B.5,

$$\begin{aligned} \beta^T &= 2\sigma^2 + 8\sigma^2 (d_{\mathcal{X}} \log(5) + 2 \log(T) + \log(4) + \log(\det(\Sigma^T) \det(\Sigma^0)^{-1})) \\ &\leq 16\sigma^2 (d_{\mathcal{X}} + \log(T) + \log(\det(\Sigma^T) \det(\Sigma^0)^{-1})). \end{aligned} \tag{B.2}$$

In particular, we can take $C_1 = 16$ in LC³. Also,

$$\mathbb{E}[\beta^T] \leq 16\sigma^2 (d_{\mathcal{X}} + \log(T) + \gamma_T(\lambda)). \tag{B.3}$$

using the definition of the information gain.

We now conclude the proof our first main theorem (Theorem 3.2).

Proof of Theorem 3.2. Using the per-episode regret bound (Lemma B.4), our confidence ball, failure probability bound (Lemma B.5), and that $V^t \leq V_{\max}$,

$$\begin{aligned}
\mathbb{E}[\text{REGRET}_{LC^3}] &= \mathbb{E} \left[\sum_{t=0}^{T-1} (J^t(x_0; c^t) - J^*(x_0; c^t)) \right] \\
&\leq \mathbb{E} \left[\sum_{t=0}^{T-1} \mathbb{E} [\mathbf{1}(\mathcal{E}_{t,cb}) (J^t(x_0; c^t) - J^*(x_0; c^t)) \mid \mathcal{H}_t] \right] + \sqrt{V_{\max}} \sum_{t=0}^{T-1} \mathbb{E} [\mathbf{1}(\bar{\mathcal{E}}_{t,cb})] \\
&\leq \sqrt{HV_{\max}} \sum_{t=0}^{T-1} \mathbb{E} \left[\sqrt{\frac{4\beta^t}{\sigma^2} + H} \sqrt{\mathbb{E} \left[\min \left\{ \sum_{h=0}^{H-1} \|\phi_h^t\|_{(\Sigma^t)^{-1}}^2, 1 \right\} \mid \mathcal{H}_{<t} \right]} \right] + \sqrt{V_{\max}}/2 \\
&\leq \sqrt{HV_{\max}} \sum_{t=0}^{T-1} \sqrt{\mathbb{E} \left[\frac{4\beta^t}{\sigma^2} + H \right]} \sqrt{\mathbb{E} \left[\min \left\{ \sum_{h=0}^{H-1} \|\phi_h^t\|_{(\Sigma^t)^{-1}}^2, 1 \right\} \right]} + \sqrt{V_{\max}}/2 \\
&\leq \sqrt{HV_{\max}} \sqrt{\sum_{t=0}^{T-1} \mathbb{E} \left[\frac{4\beta^t}{\sigma^2} + H \right]} \sqrt{\mathbb{E} \left[\sum_{t=0}^{T-1} \min \left\{ \sum_{h=0}^{H-1} \|\phi_h^t\|_{(\Sigma^t)^{-1}}^2, 1 \right\} \right]} + \sqrt{V_{\max}}/2 \\
&\leq \sqrt{HV_{\max}} \sqrt{T \left(\frac{4\mathbb{E}[\beta^T]}{\sigma^2} + H \right)} \sqrt{\gamma_T(\lambda)} + \sqrt{V_{\max}}/2 \\
&\leq \sqrt{HV_{\max}} \sqrt{64T(d_{\mathcal{X}} + \log(T) + \gamma_T(\lambda) + H)} \sqrt{\gamma_T(\lambda)} + \sqrt{V_{\max}}/2
\end{aligned}$$

where the third inequality use that $\mathbb{E}[ab] \leq \sqrt{\mathbb{E}[a^2]\mathbb{E}[b^2]}$; the fourth uses the Cauchy-Schwartz inequality; the penultimate step uses that β_t is non-decreasing, along with the Lemma B.6 and the definition of the information gain; and the final step uses the bound on β^T in Equation B.3. This completes the proof. \square

The proof of our second main theorem (Theorem 3.8) now follows.

Proof of Theorem 3.8. By assumption 3 on V^t and the per-episode regret lemma (Lemma B.4),

$$\begin{aligned}
\mathbf{1}(\mathcal{E}_{t,cb})V^t &\leq \alpha^2 \mathbf{1}(\mathcal{E}_{t,cb}) J^t(x_0; c^t, W^*)^2 \\
&\leq 2\alpha^2 J^*(x_0; c^t, W^*)^2 + 2\mathbf{1}(\mathcal{E}_{t,cb}) \alpha^2 \left(J^t(x_0; c^t, W^*) - J^*(x_0; c^t, W^*) \right)^2 \\
&\leq 2\alpha^2 J^*(x_0; c^t, W^*)^2 + 2\alpha^2 HV_{\max} \left(\frac{4\beta^t}{\sigma^2} + H \right) \mathbb{E} \left[\min \left\{ \sum_{h=0}^{H-1} \|\phi_h^t\|_{(\Sigma^t)^{-1}}^2, 1 \right\} \mid \mathcal{H}_{<t} \right]
\end{aligned}$$

Using this, and with Lemma B.4 and Lemma B.5, we have

$$\begin{aligned}
& \mathbb{E} [\text{REGRET}_{LC^3}] \\
& \leq \mathbb{E} \left[\sum_{t=0}^{T-1} \mathbb{E} [\mathbf{1}(\mathcal{E}_{t,cb}) (J^t(x_0; c^t) - J^*(x_0; c^t)) \mid \mathcal{H}_t] \right] + \sqrt{V_{\max}} \sum_{t=0}^{T-1} \mathbb{E} [\mathbf{1}(\bar{\mathcal{E}}_{t,cb})] \\
& \leq \sum_{t=0}^{T-1} \mathbb{E} \left[\sqrt{H \mathbf{1}(\mathcal{E}_{t,cb}) V^t \left(\frac{4\beta^t}{\sigma^2} + H \right)} \sqrt{\mathbb{E} \left[\min \left\{ \sum_{h=0}^{H-1} \|\phi_h^t\|_{(\Sigma^t)^{-1}}^2, 1 \right\} \mid \mathcal{H}_{<t} \right]} \right] + \sqrt{V_{\max}}/2 \\
& \leq \alpha J^* \sqrt{2H} \sum_{t=0}^{T-1} \mathbb{E} \left[\sqrt{\frac{4\beta^t}{\sigma^2} + H} \sqrt{\mathbb{E} \left[\min \left\{ \sum_{h=0}^{H-1} \|\phi_h^t\|_{(\Sigma^t)^{-1}}^2, 1 \right\} \mid \mathcal{H}_{<t} \right]} \right] \\
& + \alpha \sqrt{2H^2 V_{\max}} \sum_{t=0}^{T-1} \mathbb{E} \left[\left(\frac{4\beta^t}{\sigma^2} + H \right) \mathbb{E} \left[\min \left\{ \sum_{h=0}^{H-1} \|\phi_h^t\|_{(\Sigma^t)^{-1}}^2, 1 \right\} \mid \mathcal{H}_{<t} \right] \right] + \sqrt{V_{\max}}/2.
\end{aligned}$$

where we have used that $\sqrt{a+b} \leq \sqrt{a} + \sqrt{b}$ for positive a and b in the last inequality.

An identical argument to that in the proof of Theorem 3.2 leads to the first term above being bounded as:

$$\begin{aligned}
& \alpha J^* \sqrt{2H} \sum_{t=0}^{T-1} \mathbb{E} \left[\sqrt{\frac{4\beta^t}{\sigma^2} + H} \sqrt{\mathbb{E} \left[\min \left\{ \sum_{h=0}^{H-1} \|\phi_h^t\|_{(\Sigma^t)^{-1}}^2, 1 \right\} \mid \mathcal{H}_{<t} \right]} \right] \\
& \leq \alpha J^* \sqrt{128\gamma_T(\lambda) (d_{\mathcal{X}} + \log(T) + \gamma_T(\lambda) + H) HT}
\end{aligned}$$

For the second term,

$$\begin{aligned}
& \mathbb{E} \left[\sum_{t=0}^{T-1} \left(\frac{4\beta^t}{\sigma^2} + H \right) \mathbb{E} \left[\min \left\{ \sum_{h=0}^{H-1} \|\phi_h^t\|_{(\Sigma^t)^{-1}}^2, 1 \right\} \mid \mathcal{H}_{<t} \right] \right] \\
& = \mathbb{E} \left[\sum_{t=0}^{T-1} \left(\frac{4\beta^t}{\sigma^2} + H \right) \min \left\{ \sum_{h=0}^{H-1} \|\phi_h^t\|_{(\Sigma^t)^{-1}}^2, 1 \right\} \right] \\
& \leq \mathbb{E} \left[\left(\frac{4\beta^T}{\sigma^2} + H \right) \sum_{t=0}^{T-1} \min \left\{ \sum_{h=0}^{H-1} \|\phi_h^t\|_{(\Sigma^t)^{-1}}^2, 1 \right\} \right] \\
& \leq 2\mathbb{E} \left[\left(\frac{4\beta^T}{\sigma^2} + H \right) \log (\det(\Sigma^T) \det(\Sigma^0)^{-1}) \right] \\
& \leq 128\mathbb{E} [(d_{\mathcal{X}} + \log(T) + \log (\det(\Sigma^T) \det(\Sigma^0)^{-1}) + H) \log (\det(\Sigma^T) \det(\Sigma^0)^{-1})] \\
& \leq 128 (H + d_{\mathcal{X}} + \log(T)) \gamma_T(\lambda) + 128\gamma_{2,T}(\lambda)
\end{aligned}$$

where we have used that β^t is measurable with respect to $\mathcal{H}_{<t}$ in the first equality; that β^t is non-decreasing in the first inequality; Lemma B.6 in the second inequality; our bound on β^T in Equation B.2 in the third inequality; and the definition of $\gamma_T(\lambda)$ and $\gamma_{2,T}(\lambda)$ in the final step.

The proof is completed via substitution. \square

B.3 Confidence Bound and Potential Function Analysis

Proof of Lemma B.5. The center of the confidence ball, \bar{W}^t , is the minimizer of the ridge regression objective in Equation 3.1; its closed-form expression is:

$$\bar{W}^t := \sum_{\tau=0}^{t-1} \sum_{h=0}^{H-1} x_{h+1}^\tau (\phi_h^\tau)^\top (\Sigma^t)^{-1},$$

where $\Sigma^t = \lambda I + \sum_{\tau=0}^{t-1} \sum_{h=0}^{H-1} \phi_h^\tau (\phi_h^\tau)^\top$. Using that $x_{h+1}^\tau = W^* \phi_h^\tau + \epsilon_h^\tau$ with $\epsilon_h^\tau \sim \mathcal{N}(0, \sigma^2 I)$,

$$\begin{aligned} \bar{W}^t - W^* &= \sum_{\tau=0}^{t-1} \sum_{h=0}^{H-1} x_{h+1}^\tau (\phi_h^\tau)^\top (\Sigma^t)^{-1} - W^* \\ &= \sum_{\tau=0}^{t-1} \sum_{h=0}^{H-1} (W^* \phi_h^\tau + \epsilon_h^\tau) (\phi_h^\tau)^\top (\Sigma^t)^{-1} - W^* \\ &= W^* \left(\sum_{\tau=0}^{t-1} \sum_{h=0}^{H-1} \phi_h^\tau (\phi_h^\tau)^\top \right) (\Sigma^t)^{-1} - W^* + \sum_{\tau=0}^{t-1} \sum_{h=0}^{H-1} \epsilon_h^\tau (\phi_h^\tau)^\top (\Sigma^t)^{-1} \\ &= -\lambda W^* (\Sigma^t)^{-1} + \sum_{\tau=0}^{t-1} \sum_{h=0}^{H-1} \epsilon_h^\tau (\phi_h^\tau)^\top (\Sigma^t)^{-1}. \end{aligned}$$

For any $0 < \delta_t < 1$, using Lemma C.4, it holds with probability at least $1 - \delta_t$,

$$\begin{aligned} \left\| (\bar{W}^t - W^*) (\Sigma^t)^{1/2} \right\|_2 &\leq \left\| \lambda W^* (\Sigma^t)^{-1/2} \right\|_2 + \left\| \sum_{\tau=0}^{t-1} \sum_{h=0}^{H-1} \epsilon_h^\tau (\phi_h^\tau)^\top (\Sigma^t)^{-1/2} \right\|_2 \\ &\leq \sqrt{\lambda} \|W^*\|_2 + \sigma \sqrt{8d_{\mathcal{X}} \log(5) + 8 \log(\det(\Sigma^t) \det(\Sigma^0)^{-1} / \delta_t)}. \end{aligned}$$

where we have also used the triangle inequality. Therefore, $\Pr(\bar{\mathcal{E}}_{t,cb}) \leq \delta_t$.

We seek to bound $\sum_{t=0}^{\infty} \Pr(\bar{\mathcal{E}}_{t,cb})$. Due to that at $t = 0$ we have initialized BALL⁰ to contain W^* , we have $\Pr(\bar{\mathcal{E}}_{0,cb}) = 0$. For $t \geq 1$, let us assign failure probability $\delta_t = (3/\pi^2)/t^2$ for the t -th event, which, using the above, gives us an upper bound on the sum failure probability as $\sum_{t=1}^{\infty} \Pr(\bar{\mathcal{E}}_{t,cb}) < \sum_{t=1}^{\infty} (1/t^2)(3/\pi^2) = 1/2$. This completes the proof. \square

Proof of Lemma B.6. Recall that $\Sigma^{t+1} = \Sigma^t + \sum_{h=0}^{H-1} \phi_h^t (\phi_h^t)^\top$ and $\Sigma^0 = \lambda I$. First use $x \leq 2 \log(1+x)$ for $x \in [0, 1]$, we have:

$$\min \left\{ \sum_{h=0}^{H-1} \|\phi_h^t\|_{(\Sigma^t)^{-1}}^2, 1 \right\} \leq 2 \log \left(1 + \sum_{h=0}^{H-1} \|\phi_h^t\|_{(\Sigma^t)^{-1}}^2 \right).$$

For Σ^{t+1} , using its recursive formulation, we have:

$$\log \det(\Sigma^{t+1}) = \log \det(\Sigma^t) + \log \det \left(I + (\Sigma^t)^{-1/2} \sum_{h=0}^{H-1} \phi_h^t (\phi_h^t)^\top (\Sigma^t)^{-1/2} \right)$$

Denote the eigenvalues of $(\Sigma^t)^{-1/2} \sum_{h=0}^{H-1} \phi_h^t (\phi_h^t)^\top (\Sigma^t)^{-1/2}$ as σ_i for $i \geq 1$. We have

$$\log \det \left(I + (\Sigma^t)^{-1/2} \sum_{h=0}^{H-1} \phi_h^t (\phi_h^t)^\top (\Sigma^t)^{-1/2} \right) = \log \prod_{i \geq 1} (1 + \sigma_i) \geq \log \left(1 + \sum_{i \geq 1} \sigma_i \right),$$

where the last inequality uses that $\sigma_i \geq 0$ for all i . Using the above and the definition of the trace,

$$\begin{aligned} \log \det \left(I + (\Sigma^t)^{-1/2} \sum_{h=0}^{H-1} \phi_h^t (\phi_h^t)^\top (\Sigma^t)^{-1/2} \right) &\geq \log \left(1 + \text{tr} \left((\Sigma^t)^{-1/2} \sum_{h=0}^{H-1} \phi_h^t (\phi_h^t)^\top (\Sigma^t)^{-1/2} \right) \right) \\ &= \log \left(1 + \sum_{h=0}^H (\phi_h^t)^\top (\Sigma^t)^{-1} \phi_h^t \right) \end{aligned}$$

By telescoping the sum,

$$\begin{aligned} 2 \sum_{t=0}^{T-1} \log \left(1 + \sum_{h=0}^H (\phi_h^t)^\top (\Sigma^t)^{-1} \phi_h^t \right) &\leq 2 \sum_{t=1}^{T-1} (\log \det (\Sigma^{t+1}) - \log \det (\Sigma^t)) \\ &= \log (\det (\Sigma^T) \det (\Sigma^0)^{-1}), \end{aligned}$$

which completes the proof. \square

C Technical Lemmas

Lemma C.1 (Chi Squared Distance Between Two Gaussians). *For Gaussian distributions $\mathcal{N}(\mu_1, \sigma^2 I)$ and $\mathcal{N}(\mu_2, \sigma^2 I)$, the (squared) chi-squared distance between \mathcal{N}_1 and \mathcal{N}_2 is:*

$$\int \frac{(\mathcal{N}_1(z) - \mathcal{N}_2(z))^2}{\mathcal{N}_1(z)} dz = \exp \left(\frac{\|\mu_1 - \mu_2\|^2}{2\sigma^2} \right) - 1$$

Proof. Observe that:

$$\int \frac{(\mathcal{N}_1(z) - \mathcal{N}_2(z))^2}{\mathcal{N}_1(z)} dz = \int \mathcal{N}_1(z) - 2\mathcal{N}_2(z) + \frac{\mathcal{N}_2(z)^2}{\mathcal{N}_1(z)} dz = -1 + \int \frac{\mathcal{N}_2(z)^2}{\mathcal{N}_1(z)} dz.$$

Note that for $\mathcal{N}_2^2(z)/\mathcal{N}_1(z)$, we have:

$$\mathcal{N}_2^2(z)/\mathcal{N}_1(z) = \frac{1}{Z} \exp \left(-\frac{1}{2\sigma^2} (2\|z - \mu_2\|_2^2 - \|z - \mu_1\|_2^2) \right),$$

where Z is the normalization constant for $\mathcal{N}(0, \sigma^2 I)$, i.e. $Z = \int \exp \left(-\frac{1}{2\sigma^2} \|z\|_2^2 \right) dz$.

For $2\|z - \mu_2\|_2^2 - \|z - \mu_1\|_2^2$, we can verify that:

$$2\|z - \mu_2\|_2^2 - \|z - \mu_1\|_2^2 = \|z + (\mu_1 - 2\mu_2)\|_2^2 - 2\|\mu_1 - \mu_2\|_2^2.$$

This implies that:

$$\begin{aligned}
\int \frac{\mathcal{N}_2(z)^2}{\mathcal{N}_1(z)} dz &= \frac{1}{Z} \int \exp\left(-\frac{1}{2\sigma^2} (\|z - (2\mu_2 - \mu_1)\|_2^2 - 2\|\mu_1 - \mu_2\|)\right) dz \\
&= \frac{1}{Z} \exp\left(\frac{\|\mu_1 - \mu_2\|_2^2}{\sigma^2}\right) \int \exp\left(-\frac{1}{2\sigma^2} \|z - (2\mu_2 - \mu_1)\|_2^2\right) dz \\
&= \exp\left(\frac{\|\mu_1 - \mu_2\|_2^2}{\sigma^2}\right),
\end{aligned}$$

which concludes the proof. \square

Lemma C.2 (Expectation Difference Under Two Gaussians). *For Gaussian distribution $\mathcal{N}(\mu_1, \sigma^2 I)$ and $\mathcal{N}(\mu_2, \sigma^2 I)$, and for any (appropriately measurable) positive function g , it holds that:*

$$\mathbb{E}_{z \sim \mathcal{N}_1}[g(z)] - \mathbb{E}_{z \sim \mathcal{N}_2}[g(z)] \leq \min\left\{\frac{\|\mu_1 - \mu_2\|}{\sigma}, 1\right\} \sqrt{\mathbb{E}_{z \sim \mathcal{N}_1}[g(z)^2]}.$$

Proof. Define $m_i = \mathbb{E}_{z \sim \mathcal{N}_i}[g(z)]$ for $i \in \{0, 1\}$. We have:

$$\begin{aligned}
m_1 - m_2 &= \mathbb{E}_{z \sim \mathcal{N}_1}\left[g(z) \left(1 - \frac{\mathcal{N}_2(z)}{\mathcal{N}_1(z)}\right)\right] \\
&\leq \sqrt{\mathbb{E}_{z \sim \mathcal{N}_1}[g(z)^2]} \sqrt{\int \frac{(\mathcal{N}_1(z) - \mathcal{N}_2(z))^2}{\mathcal{N}_1(z)} dz} \\
&= \sqrt{\mathbb{E}_{z \sim \mathcal{N}_1}[g(z)^2]} \sqrt{\exp\left(\frac{\|\mu_1 - \mu_2\|^2}{2\sigma^2}\right) - 1}
\end{aligned}$$

where we have used the previous chi-squared distance bound. Also since m_2 is positive,

$$m_1 - m_2 \leq m_1 \leq \sqrt{\mathbb{E}_{z \sim \mathcal{N}_1}[g(z)^2]},$$

and so

$$m_1 - m_2 \leq \sqrt{\mathbb{E}_{z \sim \mathcal{N}_1}[g(z)^2]} \sqrt{\min\left\{\exp\left(\frac{\|\mu_1 - \mu_2\|^2}{2\sigma^2}\right) - 1, 1\right\}}$$

Now if the min is not achieved by 1, then $\frac{\|\mu_1 - \mu_2\|^2}{2\sigma^2} \leq 1$. And since $\exp(x) \leq 1 + 2x$ for $0 \leq x \leq 1$, we have:

$$\min\left\{\exp\left(\frac{\|\mu_1 - \mu_2\|^2}{2\sigma^2}\right) - 1, 1\right\} \leq \min\left\{1 + \frac{\|\mu_1 - \mu_2\|^2}{\sigma^2} - 1, 1\right\} = \min\left\{\frac{\|\mu_1 - \mu_2\|^2}{\sigma^2}, 1\right\}.$$

which completes the proof. \square

Lemma C.3 (Self-Normalized Bound for Vector-Valued Martingales; [Abbasi-Yadkori et al., 2011]). Let $\{\varepsilon_i\}_{i=1}^\infty$ be a real-valued stochastic process with corresponding filtration $\{\mathcal{F}_i\}_{i=1}^\infty$ such that ε_i is \mathcal{F}_i measurable, $\mathbb{E}[\varepsilon_i|\mathcal{F}_{i-1}] = 0$, and ε_i is conditionally σ -sub-Gaussian with $\sigma \in \mathbb{R}^+$. Let $\{X_i\}_{i=1}^\infty$ be a stochastic process with $X_i \in \mathcal{H}$ (some Hilbert space) and X_i being \mathcal{F}_i measurable. Assume that a linear operator $V : \mathcal{H} \rightarrow \mathcal{H}$ is positive definite, i.e., $x^\top V x > 0$ for any $x \in \mathcal{H}$. For any t , define the linear operator $V_t = V + \sum_{i=1}^t X_i X_i^\top$ (here xx^\top denotes outer-product in \mathcal{H}). With probability at least $1 - \delta$, we have for all $t \geq 1$:

$$\left\| \sum_{i=1}^t X_i \varepsilon_i \right\|_{V_t^{-1}}^2 \leq 2\sigma^2 \log \left(\frac{\det(V_t)^{1/2} \det(V)^{-1/2}}{\delta} \right).$$

We generalize this lemma as follows:

Lemma C.4 (Self-Normalized Bound for Matrix-Valued Martingales). Let $\{\varepsilon_i\}_{i=1}^\infty$ be a d -dimensional vector-valued stochastic process with corresponding filtration $\{\mathcal{F}_i\}_{i=1}^\infty$ such that ε_i is \mathcal{F}_i measurable, $\mathbb{E}[\varepsilon_i|\mathcal{F}_{i-1}] = 0$, and ε_i is conditionally σ -sub-Gaussian with $\sigma \in \mathbb{R}^+$.¹ Let $\{X_i\}_{i=1}^\infty$ be a stochastic process with $X_i \in \mathcal{H}$ (some Hilbert space) and X_i being \mathcal{F}_i measurable. Assume that a linear operator $V : \mathcal{H} \rightarrow \mathcal{H}$ is positive definite. For any t , define the linear operator $V_t = V + \sum_{i=1}^t X_i X_i^\top$. Then, with probability at least $1 - \delta$, we have for all t , we have:

$$\left\| \sum_{i=1}^t \varepsilon_i X_i^\top V_t^{-1/2} \right\|_2^2 \leq 8\sigma^2 d \log(5) + 8\sigma^2 \log \left(\frac{\det(V_t)^{1/2} \det(V)^{-1/2}}{\delta} \right)$$

Proof. Denote $S = \sum_{i=1}^t \varepsilon_i X_i^\top$. Let us form an ϵ -net, in ℓ_2 distance, \mathcal{C} over the unit ball $\{w : \|w\|_2 \leq 1, w \in \mathbb{R}^d\}$. Via a standard covering argument (e.g. [Shalev-Shwartz and Ben-David, 2014]), we can choose \mathcal{C} such that $\log(|\mathcal{C}|) \leq d \log(1 + 2/\epsilon)$.

Consider a fixed $w \in \mathcal{C}$ and $w^\top S = \sum_{i=1}^t w^\top \varepsilon_i X_i^\top$. Note that $w^\top \varepsilon_i$ is a σ -sub Gaussian due to $\|w\|_2 \leq 1$. Hence, Lemma C.3 implies that with probability at least $1 - \delta$, for all t ,

$$\left\| V_t^{-1/2} \sum_{i=1}^t X_i (w^\top \varepsilon_i) \right\|_2 \leq \sqrt{2}\sigma \sqrt{\log \left(\frac{\det(V_t)^{1/2} \det(V)^{-1/2}}{\delta} \right)}.$$

Now apply a union bound over \mathcal{C} , we get that with probability at least $1 - \delta$:

$$\forall w \in \mathcal{C} : \left\| V_t^{-1/2} \sum_{i=1}^t X_i (w^\top \varepsilon_i) \right\|_2 \leq \sqrt{2}\sigma \sqrt{d \log(1 + 2/\epsilon) + \log \left(\frac{\det(V_t)^{1/2} \det(V)^{-1/2}}{\delta} \right)}.$$

¹We say a vector-valued, random variable z is σ -sub-Gaussian if $w \cdot z$ is σ -sub-Gaussian for every unit vector w .

For any w with $\|w\|_2 \leq 1$, there exists a $w' \in \mathcal{C}$ such that $\|w - w'\|_2 \leq \epsilon$. Hence, for all w such that $\|w\|_2 \leq 1$,

$$\begin{aligned} \left\| V_t^{-1/2} \sum_{i=1}^t X_i (w^\top \epsilon_i) \right\|_2 &\leq \sqrt{2}\sigma \sqrt{d \log(1 + 2/\epsilon) + \log\left(\frac{\det(V_t)^{1/2} \det(V)^{-1/2}}{\delta}\right)} \\ &\quad + \epsilon \left\| \sum_{i=1}^t \epsilon_i X_i^\top V_t^{-1/2} \right\|_2. \end{aligned}$$

By the definition of the spectral norm, this implies that:

$$\left\| \sum_{i=1}^t \epsilon_i X_i^\top V_t^{-1/2} \right\|_2 \leq \frac{1}{1 - \epsilon} \sqrt{2}\sigma \sqrt{d \log(1 + 2/\epsilon) + \log\left(\frac{\det(V_t)^{1/2} \det(V)^{-1/2}}{\delta}\right)}$$

Taking $\epsilon = 1/2$ concludes the proof. \square

Lemma C.5. For any sequence x_0, \dots, x_{T-1} such that, for $t < T$, $x_t \in \mathbb{R}^d$ and $\|x_t\|_2 \leq B \in \mathbb{R}^+$, we have:

$$\log \det \left(I + \frac{1}{\lambda} \sum_{t=0}^{T-1} x_t x_t^\top \right) \leq d \log \left(1 + \frac{TB^2}{d\lambda} \right).$$

Proof. Denote the eigenvalues of $\sum_{t=0}^{T-1} x_t x_t^\top$ as $\sigma_1, \dots, \sigma_d$, and note:

$$\sum_{i=1}^d \sigma_i = \text{tr} \left(\sum_{t=0}^{T-1} x_t x_t^\top \right) \leq TB^2.$$

Using the AM-GM inequality,

$$\begin{aligned} \log \det \left(I + \frac{1}{\lambda} \sum_{t=0}^{T-1} x_t x_t^\top \right) &= \log \left(\prod_{i=1}^d (1 + \sigma_i/\lambda) \right) \\ &= d \log \left(\prod_{i=1}^d (1 + \sigma_i/\lambda) \right)^{1/d} \leq d \log \left(\frac{1}{d} \sum_{i=1}^d (1 + \sigma_i/\lambda) \right) \leq d \log \left(1 + \frac{TB^2}{d\lambda} \right), \end{aligned}$$

which concludes the proof. \square

D Simulation Setups and Results

Below, we provide simulation setups, including the details of environments and parameter settings. Specifically, the hyper-parameters, namely, 1) variance of random control variation for MPPI, 2) temperature parameter for MPPI, 3) planning horizon, 4) number of planning samples, 5) prior parameter λ , 6) posterior reshaping constant, 7) number of episodes between model updates, 8) number of features, 9) RFF bandwidth, are presented.

Note parameters were tuned in the following way: we first tuned MPPI parameters on ground truth models, then we tuned number of RFFs, their bandwidth, prior parameter, and posterior reshaping constant.

Table 2: Hyper-parameters used for InvertedPendulum environment.

MPPI Hyper-parameters	Value	LC ³ Hyper-parameters	Value
variance of controls	0.2 ²	number of features	200
temperature parameter	0.1	RFF bandwidth	5.5
planning horizon	10	prior parameter	10 ⁻⁴
number of planning samples	256	posterior reshaping constant	0
		episodes between model updates	1

Table 3: Hyper-parameters used for Acrobot environment.

MPPI Hyper-parameters	Value	LC ³ Hyper-parameters	Value
variance of controls	0.2 ²	number of features	200
temperature parameter	0.3	RFF bandwidth	4.5
planning horizon	30	prior parameter	0.01
number of planning samples	256	posterior reshaping constant	10 ⁻³
		episodes between model updates	1

D.1 Gym Environments

The hyper-parameters used for InvertedPendulum, Acrobot, CartPole, Mountain Car, Reacher, and Hopper are shown in Table 2, 3, 4, 5, 6, and 7, respectively. We used `JULIA_NUM_THREADS=12` for all the Gym experiments.

We mention that we tested many heuristics to improve performance such as input normalization, different prior parameter for each output dimension, using multiple bandwidth of RFFs, ensemble of RFF models, warm start of planner, experience replay, etc., however, none of them *consistently* improved the performance across tasks. Therefore we present the results with no such heuristics in this paper. Interestingly, increasing number of RFFs for some contact-rich dynamics such as Hopper did not reduce the modeling error significantly. Being able to model some of the critical interactions such as contacts seems to be the key for the success of such a complicated environment.

Table 4: Hyper-parameters used for CartPole environment.

MPPI Hyper-parameters	Value	LC ³ Hyper-parameters	Value
variance of controls	0.2 ²	number of features	200
temperature parameter	0.1	RFF bandwidth	1.5
planning horizon	50	prior parameter	5 × 10 ⁻⁴
number of planning samples	128	posterior reshaping constant	10 ⁻⁴
		episodes between model updates	1

Table 5: Hyper-parameters used for Mountain Car environment.

MPPI Hyper-parameters	Value	LC ³ Hyper-parameters	Value
variance of controls	0.3 ²	number of features	100
temperature parameter	0.2	RFF bandwidth	1.3
planning horizon	110	prior parameter	0.01
number of planning samples	512	posterior reshaping constant	10 ⁻⁶
		episodes between model updates	1

Table 6: Hyper-parameters used for Reacher environment.

MPPI Hyper-parameters	Value	LC ³ Hyper-parameters	Value
variance of controls	0.2 ²	number of features	300
temperature parameter	0.3	RFF bandwidth	4.0
planning horizon	20	prior parameter	0.01
number of planning samples	256	posterior reshaping constant	0
		episodes between model updates	4

Table 7: Hyper-parameters used for Hopper environment.

MPPI Hyper-parameters	Value	LC ³ Hyper-parameters	Value
variance of controls	0.2 ²	number of features	200
temperature parameter	0.2	RFF bandwidth	12.0
planning horizon	128	prior parameter	0.005
number of planning samples	64	posterior reshaping constant	0.01
		episodes between model updates	1

Table 8: Hyper-parameters used for Maze environment.

Planner Hyper-parameters	Value	LC ³ Hyper-parameters	Value
variance of controls	0.3 ²	number of features	100
temperature parameter	0.05	prior parameter	0.01
MPPI planning horizon	50	posterior reshaping constant	10 ⁻³ (<i>best</i>)
MPPI planning samples	1024	episodes between model updates	1
PETS-CEM horizon	50		
PETS-CEM samples	500		
PETS-CEM elite size	50		

D.2 Maze

In the Maze environment, states and controls are continuous and the agent plans over continuous spaces; however, the dynamics is given by 1) $x_{h+1} = x_h + [-0.5, 0]^\top$ (i.e., moving one step left) if $\lceil 2u_h \rceil = -1$, 2) $x_{h+1} = x_h + [0, -0.5]^\top$ (i.e., moving one step up) if $\lceil 2u_h \rceil = 0$, 3) $x_{h+1} = x_h + [0.5, 0]^\top$ (i.e., moving one step right) if $\lceil 2u_h \rceil = 1$, and 4) $x_{h+1} = x_h + [0, 0.5]^\top$ (i.e., moving one step down) if $\lceil 2u_h \rceil = 2$, except for the case there is a wall in the direction of travel, which then ends up $x_{h+1} = x_h$.

The hyper-parameters of Maze experiments are shown in Table 8. Note the number of features is 100 because one hot vector (e.g., $\phi(x, u) = [1, 0, \dots, 0]^\top$ if $x \leq -0.75$ and $u \leq -0.5$) in this maze environment is 100 dimension. Table 8 also includes the parameters used for PETS-CEM; we used the recommended values as in the paper and the codebase, except for the planning horizon. The planning horizon was set to be the same as the MPPI counterpart. We used `JULIA_NUM_THREADS=12` for all the Maze experiments.

D.3 Armhand with Model Ensemble Features

In table 9, we list the dynamical properties that were randomized to make our ensemble. We use uniform distributions to present a window of possible, realistic values for the parameters: for example, we randomize the objects mass between 0.1 and 1.0 kg. The center of mass distributions is the deviation from the center of the sphere, while the moments of inertia parameter is one value applied to all elements of a diagonal inertia matrix for the object. The contact parameters are specific to the MuJoCo dynamics simulator we use [Todorov et al. \[2012\]](#), and are the parameters of internal contact model of the simulation. The range of values of the parameters allow for objects in the ensemble to have different softness and rebound effects.

Also, table 10 lists learned model predictive error for different features, indicating that the ensemble of MuJoCo model successfully captured the true dynamics.

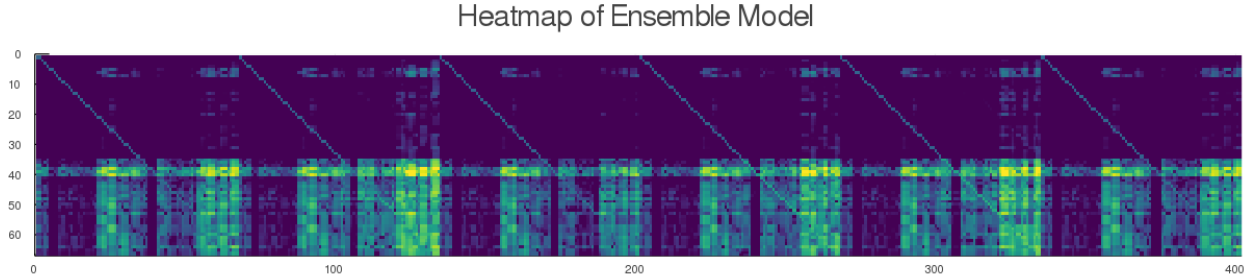


Figure 4: Here we render a representative heatmap of the learned W model from the 6 ensemble model features. Visible are 6 diagonal traces acting as a weighted average of the output of each member of the ensemble, but also significant off-diagonal values. The upper block values represent generalized positions, while the lower block is generalized velocities. Critical to modeling contact forces is accurate prediction of velocity.

Table 9: Hyper-parameters used for Armhand environment.

Hyper-parameter	Value	Ensemble Parameter	Value
variance of controls	0.2 ²	Models in Ensemble	6
temperature parameter	0.08	Mass	$\mathcal{U}(0.01, 1.0)$
planning horizon	50	Center of Mass	$\mathcal{U}(-0.04, 0.04) \times 3$
number of planning samples	64	Moments of Inertia	$\mathcal{U}(0.0001, 0.0004)$
prior parameter	0.0001	Contact Param. (solimp)	$[\mathcal{U}(0.5, 0.99),$ $\mathcal{U}(0.4, 0.98),$ $\mathcal{U}(0.0001, 0.01),$ $\mathcal{U}(0.49, 0.51),$ $\mathcal{U}(1.9, 2.1)]$
posterior reshaping constant	0.01	Contact Param. (solref)	$[\mathcal{U}(0.01, 0.03),$ $\mathcal{U}(0.9, 1.1)]$
episodes between model updates	1		

Table 10: Learned model predictive error for different features.

Feature method	Predictive Error: $\ x_{h+1} - W\phi\ _2 / \ W\phi\ _2$
Random Fourier Features, 2048	0.22
2 Layer Neural Network, 2048 hidden, <i>relu</i> activation	0.41
Model Ensemble of 6 models	0.09